DOI: 10.1002/chem.200700963

Sterically Engineered C-F Activation

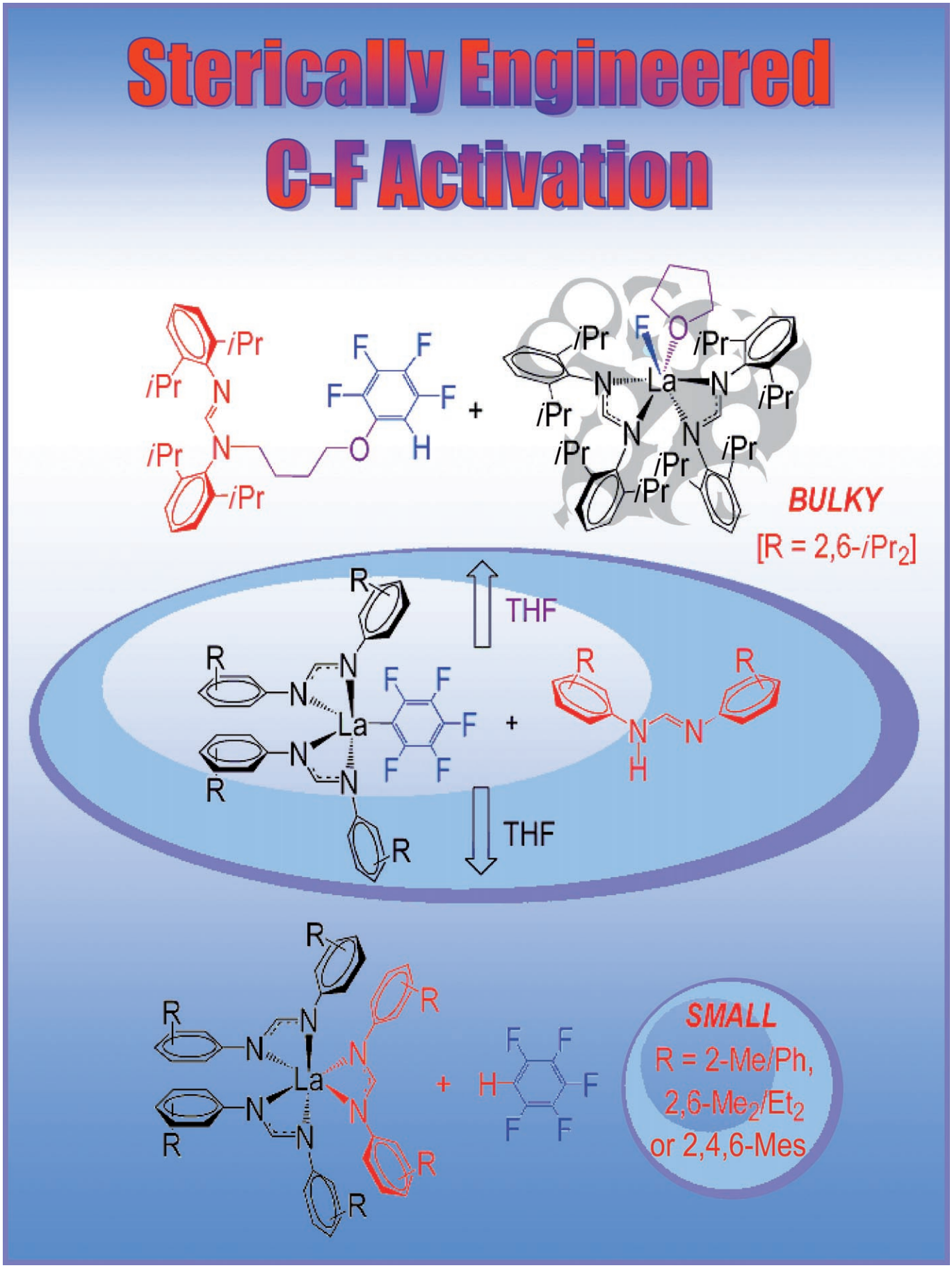

Steric Modulation of Coordination Number and Reactivity in the Synthesis of Lanthanoid(III) Formamidinates

Marcus L. Cole,[a, b] Glen B. Deacon,[a] Craig M. Forsyth,[a] Peter C. Junk,*[a] Kristina Konstas,[a] and Jun Wang[a]

Abstract: Reactions of a range of the readily prepared and sterically tunable *N,N′*-bis(aryl)formamidines with lanthanoid metals and bis(pentafluorophenyl)mercury ($Hg(C_6F_5)_2$) in THF have given an extensive series of tris(formamidinato)lanthanoid(III) complexes, $[Ln(Form)_3(thf)_n]$, namely $[La(o\text{-TolForm})_3(thf)_2]$, $[Er(o\text{-TolForm})_3(thf)]$, $[La(XylForm)_3(thf)]$, $[Sm(XylForm)_3]$, $[Ln(MesForm)_3]$ (Ln = La, Nd, Sm and Yb), $[Ln(EtForm)_3]$ (Ln = La, Nd, Sm, Ho and Yb), and $[Ln(o\text{-PhPhForm})_3]$ (Ln = La, Nd, Sm and Er). [For an explanation of the *N,N′*-bis(aryl)formamidinate abbreviations used see Scheme 1.] Analogous attempts to prepare $[Yb(o\text{-TolForm})_3]$ by this method invariably yielded $[\{Yb(o\text{-TolForm})_2(\mu\text{-OH})(thf)\}_2]$, but $[Yb(o\text{-TolForm})_3]$ was isolated from a metathesis synthesis. X-ray crystal structures show exclusively *N,N′*-chelation of the Form ligands and a gradation in coordination number with Ln^{3+} size and with Form ligand bulk. The largest ligands, MesForm, EtForm and *o*-PhPhForm give solely homoleptic complexes, the first two being six-coordinate, the last having an η^1-π-Ar–Ln interaction. Reaction of lanthanoid elements and $Hg(C_6F_5)_2$ with the still bulkier DippFormH in THF resulted in C–F activation and formation of $[Ln(DippForm)_2F(thf)]$ (Ln = La, Ce, Nd, Sm and Tm) complexes, and $o\text{-}HC_6F_4O(CH_2)_4DippForm$ in which the formamidine is functionalised by a ring-opened THF that has trapped tetrafluorobenzyne. Analogous reactions between Ln metals, $Hg(o\text{-}HC_6F_4)_2$ and DippFormH yielded $[Ln(DippForm)_2F(thf)]$ (Ln = La, Sm and Nd) and $3,4,5\text{-}F_3C_6H_2O(CH_2)_4DippForm$. X-ray crystal structures of the heteroleptic fluorides show six-coordinate monomers with two chelating DippForm ligands and *cisoid* fluoride and THF ligands in a trigonal prismatic array. The organometallic species $[Ln(DippForm)_2(C{\equiv}CPh)(thf)]$ (Ln = Nd or Sm) are obtained from reaction of Nd metal, bis(phenylethynyl)mercury ($Hg(C{\equiv}CPh)_2$) and DippFormH, and the oxidation of $[Sm(DippForm)_2(thf)_2]$ with $Hg(C{\equiv}CPh)_2$, respectively. The monomeric, six-coordinate, *cisoid* $[Ln(DippForm)_2(C{\equiv}CPh)(thf)]$ complexes have trigonal prismatic geometries and rare (for Ln) terminal C≡CPh groups with contrasting Ln–C≡C angles (Ln = Nd, 170.9(4)°; Ln = Sm, 142.9(7)°). Their formation lends support to the view that $[Ln(DippForm)_2F(thf)]$ complexes arise from oxidative formation and C–F activation of $[Ln(DippForm)_2(C_6F_5)]$ intermediates.

Keywords: C–F activation · formamidinates · lanthanides · steric engineering · structure elucidation

Introduction

Amidinates ($[R^1NC(R^2)NR^3]^-$) and guanidinates ($[R^1NC(NR^2)NR^3]^-$ (R^n = alkyl, aryl or organosilyl) have found a role as tunable alternatives to the ubiquitous cyclopentadienyl family of ligands.[1] They are generally prepared as alkali metal derivatives by addition of a metal alkyl/aryl/diorganoamide reagent to a commercially available 1,3-disubstituted carbodiimide,[2] or by a 1,3-silyl shift of an in-situ-generated alkali metal imide.[3] There have been few attempts to isolate the corresponding neutral amidines or guanidines from these preparations. For this reason, the reaction of alkali metal precursors[4] with rare earth halides constitutes the traditional means of accessing rare earth amidinates and guanidinates.[1,5] Metal-based syntheses,[6] which typically require a neutral ligand precursor, have been little explored as an alternative.

The *N,N′*-bis(aryl)formamidines, ArN=CH–NHAr (Ar = aryl), are an uncharged amidine subfamily that is readily

[a] Dr. M. L. Cole, Prof. G. B. Deacon, Dr. C. M. Forsyth, Prof. P. C. Junk, Dr. K. Konstas, Dr. J. Wang
School of Chemistry, Monash University
Victoria 3800 (Australia)
Fax: (+61) 3-9905-4597
E-mail: peter.junk@sci.monash.edu.au

[b] Dr. M. L. Cole
School of Chemistry and Physics, University of Adelaide
Adelaide, South Australia 5005 (Australia)

prepared by the condensation of a substituted aniline with triethyl orthoformate.[7] Modification of the aryl group to permit steric tuning is straightforward, making *N,N′*-bis-(aryl)formamidines a convenient class of ligand for both metal-based synthesis[6] and the study of steric effects in structural rare earth chemistry. Accordingly, we have targeted tris(formamidinato)lanthanoid(III) complexes to examine the influence of steric modulation on coordination number and geometry, and to test the versatility of the increasingly competitive redox transmetallation/ligand exchange synthesis from the rare earth element, bis(pentafluorophenyl)mercury (or other diarylmercurials) and a neutral protic ligand [Eq. (1)].[6a,b] The method has the advantage over metathesis of simplicity of workup and avoidance of alkali metal retention.

$$2\,\mathrm{Ln} + n\,\mathrm{Hg(C_6F_5)_2} + 2n\,\mathrm{LH} \xrightarrow[n=2,3]{} 2\,[\mathrm{LnL}_n] + n\,\mathrm{Hg} + 2n\,\mathrm{C_6F_5H} \quad (1)$$

Only one tris(formamidinato)lanthanoid(III) complex has been reported previously, namely, [Sm(DippForm)$_3$], (DippFormH = *N,N′*-bis(2,6-diisopropylphenyl)formamidine), which was prepared unexpectedly by solvent induced rearrangement of [Na(thf)$_5$][Sm(DippForm)$_2$I$_2$(thf)].[8]

The synthetic possibilities of the redox transmetallation/ligand exchange [Eq. (1)] are not restricted to the formation of [LnL$_n$] complexes. For instance, the last two steps in the preparation of [LnL$_3$] complexes are considered to be the reactions given in Equations (2) and (3).[6a,9]

$$2\,[\mathrm{LnL_2}] + \mathrm{Hg(C_6F_5)_2} \rightarrow 2\,[\mathrm{LnL_2(C_6F_5)}] + \mathrm{Hg} \quad (2)$$

$$[\mathrm{LnL_2(C_6F_5)}] + \mathrm{LH} \rightarrow [\mathrm{LnL_3}] + \mathrm{C_6F_5H} \quad (3)$$

If LH is bulky, the reaction in Equation (3) can be inhibited or slowed to provide scope for C–F activation of the [LnL$_2$(C$_6$F$_5$)] intermediate to give a fluoride ([LnL$_2$F]) and tetrafluorobenzyne [Eq. (4)]. (Alternatively if redox transmetallation directly gives a Ln(C$_6$F$_5$)$_3$ intermediate, incomplete protolysis can give the [Ln(Form)$_2$(C$_6$F$_5$)] intermediate.)

$$[\mathrm{LnL_2(C_6F_5)}] \rightarrow [\mathrm{LnL_2F}] + o\text{-}\mathrm{C_6F_4} \quad (4)$$

In preliminary studies we have successfully prepared [La(DippForm)$_2$F(thf)] from elemental lanthanum, Hg(C$_6$F$_5$)$_2$ and the bulky *N,N′*-bis(aryl)formamidine DippFormH,[10] and shown that the samarium analogue can be accessed from the divalent precursor [Sm(DippForm)$_2$(thf)$_2$] and Hg(C$_6$F$_5$)$_2$ in THF [Eq. (5)].[8] This highlights the steric influence of the donor solvent (THF), which further frustrates the final protolysis, contrary to the aforementioned redistribution of [Na(thf)$_5$][Sm(DippForm)$_2$I$_2$(thf)] to [Sm(DippForm)$_3$] and [SmI$_3$(thf)$_{3.5}$] upon dissolution in toluene. Likewise, protolysis of [Lu(OAr)$_2$(CCPh)(thf)$_2$] by HOAr (OAr = OC$_6$H$_2$-2,6-*t*Bu$_2$-4-OMe) to give [Lu(OAr)$_3$] proceeds in C$_6$D$_6$, but not deutero-tetrahydrofuran.[9]

$$2[\mathrm{Sm(DippForm)_2(thf)_2}] + \mathrm{Hg(C_6F_5)_2} \xrightarrow{\mathrm{THF}} 2[\mathrm{Sm(DippForm)_2F(thf)}] + \mathrm{Hg} + 2\,o\text{-}\mathrm{C_6F_4} \quad (5)$$

Heteroleptic rare earth fluorides remain an extremely limited class[11–13] that is typically accessed by oxidative C–F activation by using a divalent lanthanoid species[12] or treatment of trivalent precursors, for example, [LnCp$_3$], with a masked source of HF.[13a] Thus, new synthetic approaches, particularly those that do not require a divalent lanthanoid starting material,[14] command considerable interest.

We now report the syntheses and structures of a range of sterically varied heteroleptic and homoleptic tris(formamidinato)lanthanoid(III) complexes by redox transmetallation/ligand exchange. In addition, we report the sterically engineered synthesis of several fluorobis(formamidinato)lanthanoid(III) complexes, plausibly involving C–F activation of a [LnL$_2$(C$_6$F$_5$)] intermediate [Eq. (4)] and analogous syntheses utilising bis(2,3,4,5-tetrafluorophenyl)mercury, together with the isolation of N-functionalised *N,N′*-bis(aryl)formamidines by trapping of the polyfluorobenzyne co-product of the reaction given in Equation (4). Furthermore, use of bis(phenylethynyl)mercury in place of Hg(C$_6$F$_5$)$_2$ yields the organometallic products [Ln(DippForm)$_2$(CCPh)(thf)] (Ln = Nd and Sm) providing support for the organometallic intermediates proposed in Equations (2) and (3).

Results and Discussion

Synthesis and spectroscopic characterisation

[Ln(Form)$_3$(thf)$_n$] complexes: Redox transmetallation/ligand exchange reactions between an excess of lanthanoid metal, bis(pentafluorophenyl)mercury and an *N,N′*-bis(aryl)-formamidine (FormH), namely *N,N′*-bis(*o*-tolyl)formamidine (*o*-TolFormH), *N,N′*-bis(2,6-dimethylphenyl)formamidine (XylFormH), *N,N′*-bis(2,4,6-trimethylphenyl)formamidine (MesFormH), *N,N′*-bis(2,6-diethylphenyl)formamidine (EtFormH) and *N,N′*-bis(*o*-phenylphenyl)formamidine (*o*-PhPhFormH), in THF yield the tris(formamidinato)lanthanoid(III) complexes [Ln(Form)$_3$(thf)$_n$]; **1La**, **1Er**, **2La**, **2Sm**, **3La**, **3Nd**, **3Sm**, **3Yb**, **4La**, **4Nd**, **4Sm**, **4Ho**, **4Yb**, **5La**, **5Nd**, **5Sm**, **5Er** (Table 1 and Scheme 1) generally in good yield [Eq. (6), R = C$_6$F$_5$].

$$2\,\mathrm{Ln} + 3\,\mathrm{HgR_2} + 6\,\mathrm{FormH} \xrightarrow[n=0-2]{\mathrm{THF}} 2\,[\mathrm{Ln(Form)_3(thf)}_n]\ (\mathbf{1}-\mathbf{5}\,\mathbf{Ln}) + 6\,\mathrm{RH} + 3\,\mathrm{Hg} \quad (6)$$

Surprisingly, attempts to prepare [Yb(*o*-TolForm)$_3$(thf)] (**1Yb**) under the same conditions consistently gave a modest yield (20%) of [{Yb(*o*-TolForm)$_2$(μ-OH)(thf)}$_2$] (**1YbOH**), plausibly from adventitious water. Complex **1Yb** was successfully obtained by salt elimination from in situ prepared lithium *N,N′*-bis(*o*-tolyl)formamidinate[4] and YbCl$_3$ [Eq. (7)].

Table 1. List of compounds and summary physical and spectroscopic of data.

		Yield [%]	M.p. [°C]	^{1}H NMR NC(**H**)N [ppm]	^{13}C NMR N**C**(H)N [ppm]	IR ν NCN [cm^{-1}]	IR γCH[a] [cm^{-1}]
[La(*o*-TolForm)$_3$(thf)$_2$]·2.5 THF	**1La**	89	160–162	8.64	165.0	1667 (m)	757 (m–s)
[Er(*o*-TolForm)$_3$]·THF	**1Er**	38	183–186	–		1668 (s)	755 (s)
[{Yb(*o*-TolForm)$_2$(μ-OH)(thf)}$_2$]·2 THF	**1YbOH**	20	200	–		1667 (m)	757 (m)
[Yb(*o*-TolForm)$_3$(thf)]	**1Yb**	72	142–144	−7.01		1667 (m)	753 (s)
[La(XylForm)$_3$(thf)]·2 THF	**2La**	86	218–220	8.01	169.8	1651 (m–s)	762 (s)
[Sm(XylForm)$_3$]	**2Sm**	80	294–298	10.92	190.8	1651 (m–s)	762 (s)
[La(MesForm)$_3$]·2 THF	**3La**	87	256–260	8.15	170.1	1652 (m)	850 (m)[b]
[Nd(MesForm)$_3$]·2 toluene	**3Nd**	65	318–320	9.03	169.9	1645 (m)	851 (m)[b]
[Sm(MesForm)$_3$]	**3Sm**	71	200–204	11.11	191.8	1646 (m)	851 (s)[b]
[Yb(MesForm)$_3$]	**3Yb**	81	280–284	−6.26	169.1	1640 (m)	851 (m–s)[b]
[La(EtForm)$_3$]·2 THF	**4La**	82	228–232	8.39	169.2	1667 (m)	756 (s)
[Nd(EtForm)$_3$]·2 THF	**4Nd**	77	156–160	8.21	172.2	1665 (m–s)	756 (s)
[Sm(EtForm)$_3$]·2 THF	**4Sm**	88	258–260	11.31	192.4	1667 (m)	757 (s)
[Ho(EtForm)$_3$]·2 THF	**4Ho**	33	160–162	–	–	1646 (s)	757 (m–s)
[Yb(EtForm)$_3$]·2 THF	**4Yb**	38	>360	−3.75	167.9	1666 (s)	757 (s)
[La(*o*-PhPhForm)$_3$]	**5La**	70	262–266	–	–	1664 (s)	757 (s)
[Nd(*o*-PhPhForm)$_3$]	**5Nd**	73	248–252	–	–	1662 (s)	761 (m)
[Sm(*o*-PhPhForm)$_3$]·toluene	**5Sm**	82	248–252	–	–	1664 (s)	757 (s)
[Er(*o*-PhPhForm)$_3$]·toluene	**5Er**	86	260–264	–	–	1664 (s)	760 (s)
[La(DippForm)$_2$F(thf)]·toluene	**6La**[10]	84[c]	284 (decomp)	8.23	166.7	1662 (s)	759 (s)
[Ce(DippForm)$_2$F(thf)]·toluene	**6Ce**	39	273 (decomp)	–	–	1668 (s)	756 (s)
[Nd(DippForm)$_2$F(thf)]·toluene and non-solvate	**6Nd**	69[c]	276 (decomp)	−9.97		1662 (s)	757 (m)
[Sm(DippForm)$_2$F(thf)]	**6Sm**[10]	62[c]	276–278 (decomp)	overlap	–	1651 (s)	763 (s)
[Tm(DippForm)$_2$F(thf)]	**6Tm**	33	279 (decomp)	–	–	1661 (s)	756 (s)
[Nd(DippForm)$_2$(CCPh)(thf)]·toluene	**9Nd**	37	161	20.48	177.7	1667 (m)	756 (m)
[Sm(DippForm)$_2$(CCPh)(thf)]·toluene	**9Sm**	77	118–122	12.04	–	1666 (m)	755 (m)

[a] γ(CH) 1,2-disubstitution of aromatic protons. [b] γ(CH) isolated 3,5 aromatic protons. [c] Highest yield of several methods employed.

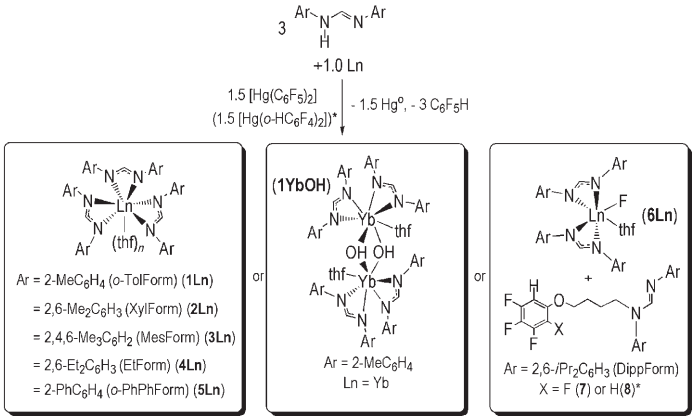

Scheme 1. Reagents and conditions: 2 equiv *o*-TolFormH, 1.5 equiv Hg(C_6F_5)$_2$ excess Ln (La, Er), THF, RT, 72 h, −1 Hg, −2 C_6F_5H (**1La**); 2 equiv *o*-TolFormH, 1 equiv Hg(C_6F_5)$_2$ excess Ln, THF, RT, 24 h, −1 Hg, −2 C_6F_5H, (**1Er**, **1YbOH**); 2 equiv XylFormH, 1.5 equiv Hg(C_6F_5)$_2$, excess La, THF, RT, 72 h, −1 Hg, −2 C_6F_5H (**2La**); 2 equiv XylFormH, 1.5 equiv Hg(C_6F_5)$_2$, excess Sm, THF, RT, 72 h, −1 Hg, −2 C_6F_5H (**2Sm**); 2 equiv MesFormH, 1.5 equiv Hg(C_6F_5)$_2$ (1 equiv for **3Sm**), excess Ln (Ln = La, Nd, Sm, Yb), THF, RT, 72 h, −1 Hg, −2 C_6F_5H (**3La**, **3Nd**, **3Sm**, **3Yb**); 2 equiv EtFormH, 1.5 equiv Hg(C_6F_5)$_2$, excess La, Sm, Nd, Ho, Yb, THF, RT, 72 h, −1 Hg, −2 C_6F_5H (**4La**, **4Nd**, **4Sm**, **4Ho**, **4Yb**); 2 equiv *o*-PhPhFormH, 1.5 equiv Hg(C_6F_5)$_2$, excess La, Sm, Nd, Er, THF, RT, 72 h, −1 Hg, −2 C_6F_5H (**5La**, **5Nd**, **5Sm**, **5Er**). (See Results and Discussion, for an explanation of the actual stoichiometry used).

$$YbCl_3 + 3\,Li(o\text{-TolForm}) \xrightarrow{THF} [Yb(o\text{-TolForm})_3(thf)]\ (\mathbf{1Yb}) + 3\,LiCl \quad (7)$$

Most syntheses, with the exception of those for **1Er**, **1YbOH** and **3Sm**, were carried out with a Hg(C_6F_5)$_2$:FormH ratio of 1:1.5 rather than the stoichiometric 1:2 [Eq. (6)] to optimise the possibility of formation, and C–F activation, of a [LnL_2(C_6F_5)] intermediate [Eqs. (2) and (4)]. Nevertheless, no [LnL_2F] complexes were formed, suggesting these *N,N′*-bis(aryl)formamidine ligands are insufficiently bulky to slow or inhibit the third protolysis step [Eq. (3)]. Thus, C–F activation [Eq. (4)] does not occur. Attempted reactions between the *N,N′*-bis(aryl)formamidine ligands XylFormH or *o*-PhPhFormH and Hg(C_6F_5)$_2$ in THF, and between ytterbium metal (the most reactive of the metal filings used) and XylFormH in THF failed, ruling out either protolysis of the mercurial or direct reaction between the metals and the *N,N′*-bis(aryl)formamidines as alternative reaction steps to those in Equations (2) and (3).

The tris(formamidinato)lanthanoid(III) complexes [Ln(Form)$_3$(thf)$_n$] obtained from the reaction in Equation (6) show variation in coordination number from 8 (n=2) to 6 (n=0) (see section on X-ray crystallographic studies). With the smallest ligand, *o*-TolForm, the lanthanum complex **1La** is eight-coordinate and the ytterbium complex **1Yb** is seven-coordinate, a result reflecting the lanthanoid contraction. With the larger XylForm ligand, the lanthanum complex **2La** is seven-coordinate, whilst the samarium analogue **2Sm** is a homoleptic six-coordinate complex. All structurally characterised complexes of the ligands MesForm, EtForm and *o*-PhPhForm are homoleptic with no THF ligands.

[Ln(DippForm)$_2$F(thf)] and associated polyfluorobenzyne-trapped co-products: Although the bulkier *N,N′*-bis(aryl)formamidinate ligands listed above are able to exclude

coligands from the coordination sphere, as illustrated by isolation of five homoleptic **4Ln** complexes as THF solvates, they are not sufficiently bulky to inhibit or slow $[LnL_3]$ formation and thereby promote C–F activation [Eq. (4)]. Accordingly, reactions with the bulkier DippFormH were examined. Using the 1:2 $Hg(C_6F_5)_2$:DippFormH mole ratio given in Equation (6), the $[Ln(DippForm)_2F(thf)]$ complexes **6La,**[10] **6Ce**, **6Nd**, **6Sm**[8] and **6Tm** were isolated, generally in good yield (Table 1 and Scheme 1), together with the trapped tetrafluorobenzyne *N,N′*-bis(2,6-diisopropylphenyl)-*N*-{4-(2′,3′,4′,5′-tetrafluorophenoxy)butyl}formamidine (**7**) as the co-product [Eq. (8), Scheme 1 for reference].

$$2\,Ln + 3\,Hg(C_6F_5)_2 + 6\,DippFormH \xrightarrow{THF} 2\,[Ln(DippForm)_2F(thf)]\ (\mathbf{6Ln}) + 3\,Hg + 4\,C_6F_5H + 2\,o\text{-}HC_6F_4O(CH_2)_4(DippForm)\ (\mathbf{7}) \quad (8)$$

When the $Hg(C_6F_5)_2$:DippFormH ratio was raised to 3:4 for Ln = La, Nd and Sm, **6La**, **6Nd** and **6Sm** were obtained in good yield without significant formation of the co-product **7**, as evidenced by ^{19}F NMR spectra of the reaction mixtures. Analogous reactions of bis(2,3,4,5-tetrafluorophenyl)-mercury and DippFormH (mole ratio 1:2) with lanthanoid metals provided **6La**, **6Nd** and **6Sm** in good yield with *N,N′*-bis(2,6-diisopropylphenyl)-*N*-{4-(3′,4′,5′-trifluorophenoxy)butyl}formamidine (**8**), isolated from trapping of a 3,4,5-trifluorobenzyne co-product. Oxidation and C–F activation using this mercurial with reduced *ortho*-fluorine substitution is noteworthy, since the oxidation potentials of mercurials are enhanced by fluorine substitution[15] (e.g. $Hg(C_6F_5)_2$ oxidises $[YbCp_2]$ but $HgPh_2$ does not),[16] reactions of ytterbium with $Hg(o\text{-}HC_6F_4)_2$ are much less clean than with $Hg(C_6F_5)_2$,[17] and C–F activation of pentafluorobenzoic acid by $[Yb(C_6F_5)_2]$[18] or $[YbCp_2]$[19] only removes one *ortho*-fluorine. Thus, the activation of a 2,3,4,5-tetrafluorophenyl substituent observed here is a significant development.

The linking of the polyfluorobenzynes through the ring opening of THF to DippForm, as per **7** and **8**, is unusual and unexpected. Tetrafluorobenzyne formed by decomposition of a pentafluorophenyl organometallic commonly inserts into $M–C_6F_5$ bonds to give a nonafluoro-2-biphenylyl organometallic compound (e.g., M = Li,[20] Sm[17]), adds a lithium halide (LiX) across the triple bond to give *o*-XC_6F_4Li,[20c] or can be trapped by furan,[17,21] benzene[21,22] or C_6D_6.[9,13c] Ring-opening of THF by $[LnL_3]$ species commonly gives alkoxolanthanoid species $[LnL_2(OCH_2CH{=}CHCH_3)]$[23] or $[LnL_2(O(CH_2)_4L)]$[24] derivatives. In the present case, we envisage that the tetrafluorobenzyne (or 2,3,4-trifluorobenzyne) from the reaction in Equation (4) (or its tetrafluorophenyl analogue) inserts into a $Ln–O_{thf}$ bond to give a zwitterionic oxoniumlanthanoidate(III) species; $[o\text{-}\{c\text{-}(CH_2)_4O^+\}C_6F_4Ln^-(DippForm)_2F]$. Ring-opening gives the carbonium lanthanoidate(III) derivative $[o\text{-}\{^+CH_2\text{-}(CH_2)_3O\}C_6F_4Ln^-(DippForm)_2F]$, which reacts with available DippFormH to give $[o\text{-}\{^+DippFormH\text{-}(CH_2)_4O\}C_6F_4Ln^-(DippForm)_2F]$. Protolysis of the Ln–C bond gives the isolated *o*-$HC_6F_4O(CH_2)_4$DippForm (**7**) (or corresponding trifluoroderivative **8**). We propose that protolysis is effected by THF rather than the hydrogen of DippFormH, since the product from reaction of La, $Hg(C_6F_5)_2$ and DippFormH in perdeuterotetrahydrofuran does not show the HC_6F_4 proton resonance at 5.96 ppm, consistent with *o*-$DC_6F_4O(CH_2)_4$DippForm formation. Protolysis of polyfluoroarylsamarium species by THF has been established during earlier labelling studies.[17]

[Ln(DippForm)$_2$(CCPh)(thf)] complexes: Since the proposed path to the heteroleptic fluorides **6Ln** involves formation and decomposition of $[Ln(DippForm)_2(C_6F_5)]$ [Eqs. (2) and (4)], it was important to establish the intermediacy of a $[Ln(DippForm)_2R]$ species utilising a mercurial for which decomposition by C–F activation [Eq. (4)] is not possible. Thus, reaction of neodymium metal, bis(phenylethynyl)mercury and DippFormH in THF resulted in the isolation of $[Nd(DippForm)_2(C{\equiv}CPh)(thf)]$ (**9Nd**) [Eq. (9)] in the presence of sufficient DippFormH to give $[Nd(DippForm)_3]$ [Eq. (6), R = C≡CPh]. This is consistent with formation of an organolanthanoid(III) intermediate in the redox transmetallation/ligand exchange process [Eq. (2)]. Furthermore, the direct analogue of equation 2 was achieved by oxidation of $[Sm(DippForm)_2(thf)_2]$[8] with $Hg(C{\equiv}CPh)_2$ to give $[Sm(DippForm)_2(C{\equiv}CPh)(thf)]$ **9Sm** [Eq. (10)].

$$2\,Nd + 3\,Hg(C{\equiv}CPh)_2 + 4\,DippFormH \xrightarrow{THF} 2\,[Nd(DippForm)_2(C{\equiv}CPh)(thf)]\ (\mathbf{9Nd}) + 3\,Hg + 4\,HC{\equiv}CPh \quad (9)$$

$$2\,[Sm(DippForm)_2(thf)_2] + Hg(C{\equiv}CPh)_2 \xrightarrow{THF} 2\,[Sm(DippForm)_2(C{\equiv}CPh)(thf)]\ (\mathbf{9Sm}) + Hg \quad (10)$$

Spectroscopic and analytical characterisation: The absence of a ν(N–H) absorption in the infrared spectra and the lack of a NH resonance in the ^1H NMR spectra of the bulk vacuum dried materials in C_6D_6 indicates complete deprotonation of the *N,N′*-bis(aryl)formamidine reagents in the isolated complexes (Table 1). Strong ν(C–N) stretching bands are observed in the region of 1670–1640 cm^{-1} for all spectra. For compound **1YbOH**, a moderate intensity ν(O–H) band is found at 3665 cm^{-1}, supporting the presence of a hydroxyl group. Prominent ring stretching modes of THF in THF-containing compounds are found in the ranges 1040–1020 and 900–800 cm^{-1}. In addition, all compounds exhibit appropriate γ(C–H) bands attributable to 1,2-, 1,2,3- and 1,2,3,5-substitution of the aromatic rings (see Table 1). Infrared spectra of the phenylethynyl compounds **9Nd** and **9Sm** display weak absorptions attributable to alkynyl stretching at 2053 and 2059 cm^{-1}. These compare well with other rare examples of lanthanoid complexes with terminal C≡CR groups,[9,24c] for example, 2082–2074 cm^{-1} for five-coordinate $[Ln(OC_6H_2\text{-}2,6\text{-}tBu_2\text{-}4\text{-}OMe)_2(CCPh)(thf)_2]$.[9]

For the diamagnetic [La(Form)$_3$(thf)$_n$] complexes, the methine resonance of the FormH ligands (6.88–7.72 ppm) is shifted to higher frequencies (Table 1). With the paramagnetic complexes, those of neodymium are similarly shifted, those of samarium to still higher frequencies, while for ytterbium complexes the shift is to negative δ values. All ^{13}C methine resonances are shifted to higher frequencies than the free ligand value ($\approx$147 ppm for all), the shift being greatest for the samarium complexes. By contrast, for the [Ln(DippForm)$_2$F(thf)] complexes, Ln = Nd and Sm, the methine proton resonance is shifted to lower frequencies, markedly in the case of Ln = Nd, but with [Nd(DippForm)$_2$(CCPh)(thf)], there is a very large shift in the opposite sense, much greater than the shift for tris(formamidinato)neodymium(III) complexes. Thus, whilst the methine resonance responds significantly to ligation, the nature of the paramagnetic shift is unpredictable. Fluoride resonances were detected for **6La**[10] and **6Sm**,[8] but lamentably could not be located for other **6Ln** complexes.

For the [Ln(Form)$_3$(thf)$_n$] complexes, compositions of bulk samples, as indicated by C,H,N,Ln analyses (or just Ln analyses), and ^{1}H NMR integrations were usually consistent with the composition of single crystals, as established by X-ray crystallography (see next section), but, in some cases, loss of solvent of crystallisation was apparent. Thus, **1La** has 2.5 THF molecules in the crystal lattice per **1La** molecular unit, but elemental analyses (particularly %La) and a ^{1}H NMR spectrum are consistent with loss of 2.5 and 1.5 lattice THF molecules, respectively. Single crystals of **3Nd** have two toluene molecules of solvation, but this was absent from the bulk product, as indicated by both ^{1}H NMR spectroscopy and elemental analyses. All five **4Ln** complexes crystallise with 2 THF of solvation, but ^{1}H NMR data and/or analyses show lattice THF is lost from the bulk samples with the exception of **4Yb**. In the case of the **6Ln** complexes, single crystals of **6La**,[10] **6Ce** and **6Nd** were obtained as toluene solvates. Lattice solvent was detected by ^{1}H NMR spectroscopy for **6La** and **6Nd**, but elemental analysis indicated lattice solvent had evaporated prior to analyses. The ready loss was particularly evident for **6Nd**, for which both a toluene solvate and the unsolvated complex were crystallographically characterised, whilst **6Sm**[8] and **6Tm** were unsolvated. Complex **6Ce** was exceptionally air sensitive, and crystals for characterisation had to be handpicked from the co-product **7** and DippFormH. The greater instability of the cerium derivative parallels that of [Ce(Odpp)$_3$] (Odpp = 2,6-diphenylphenolate)[25] and [CeCp$_3$] complexes.[26] For **9Sm**, the microanalyses indicated loss of toluene of solvation from the sample in contrast to **9Nd**.

X-ray crystallography studies

[Ln(Form)$_3$(thf)$_n$], [Ln(DippForm)$_2$F(thf)] and [Ln(DippForm)$_2$(CCPh)(thf)] complexes: Crystalline samples of compounds **1La**, **1YbOH**, **1Yb**, **2La**, **2Sm**, **3Nd**, **3Yb**, **4La**, **4Nd**, **4Sm**, **4Ho**, **4Yb**, **5Sm**, **6Ce**, **6Nd**, **6Tm**, **8**, **9Nd**, and **9Sm** of suitable quality for X-ray structure determination were grown from THF, hexane or toluene (see Experimental Section). All compounds, with the exception of **8**, were extremely air- and moisture-sensitive, and frequently prone to solvent loss (see above). All complexes are mononuclear with two or three chelating *N,N′*-bis(aryl)formamidinate ligands although other binding modes are known for these ligands[4] (see Figures 1–8, POV-RAY illustrations, 40% thermal ellipsoids), with the exception of dinuclear **1YbOH**. Table 2 contains a summary of crystallographic data for all compounds characterised by X-ray methods, while Tables 3 and 4 provide selected bond lengths and angles for compounds **1–5Ln** and **6–9Ln** (see associated reference key) with the exception of **8** (Figure 9). Diffraction data for **3Sm**

Table 2. Crystal data and refinement parameters for compounds characterised by X-ray structure determination.[a]

	1La	**1YbOH**	**1Yb**	**2La**	**2Sm**
formula	$C_{31.50}H_{40.50}La_{0.50}N_3O_{2.25}$	$C_{38}H_{47}N_4O_3Yb$	$C_{49}H_{53}N_6OYb$	$C_{63}H_{81}LaN_6O_3$	$C_{102}H_{114}N_{12}Sm_2$
M_r	566.62	780.84	915.01	1109.25	1808.75
T [K]	123(2)	123(2)	123(2)	123(2)	123(2)
space group	$I4_1/acd$	$P2_1/c$	$P\bar{1}$	$P\bar{1}$	$P2_1$
a [Å]	20.940(3)	13.218(3)	10.9199(9)	11.7821(2)	20.1506(2)
b [Å]	20.940(3)	21.210(4)	12.1899(10)	14.0546(2)	10.61290(10)
c [Å]	53.201(11)	12.686(3)	17.4497(19)	18.0375(4)	21.0118(3)
α [°]	90	90	75.429(4)	81.7590(10)	90
β [°]	90	104.33(3)	88.626(5)	83.9970(10)	91.0940(10)
γ [°]	90	90	69.956(4)	73.8760(10)	90
V [Å^3]	23328(7)	3446.1(12)	2106.9(3)	2833.16(9)	4492.69(9)
Z	32	4	2	2	2
ρ_{calcd} [g cm^{-3}]	1.291	1.505	1.442	1.300	1.337
μ [mm^{-1}]	0.785	2.756	2.264	0.804	1.348
reflections collected	52103	33360	31542	38504	52372
unique reflections	7051	8159	9728	13218	20965
parameters varied	481	423	566	700	1069
R(int)	0.0785	0.2056	0.0783	0.0398	0.0479
R_1	0.0950	0.0667	0.0637	0.0274	0.0745
wR_2	0.1449	0.1043	0.1191	0.0619	0.1763

	3Nd[a]	**3Yb**	**4La**	**4Nd**	**4Sm**
formula	$C_{142}H_{170}N_{12}Nd_2$	$C_{57}H_{69}N_6Yb$	$C_{71}H_{97}LaN_6O_2$	$C_{71}H_{97}N_6NdO_2$	$C_{71}H_{97}N_6SmO_2$
M_r	2333.38	1011.22	1205.46	1210.79	1216.90
T [K]	123(2)	123(2)	123(2)	123(2)	123(2)
space group	*C2/c*	$P2_1/n$	$P\bar{1}$	$P\bar{1}P\bar{1}$	
a [Å]	40.870(3)	9.7832(2)	12.478(3)	12.4787(6)	12.4814(2)
b [Å]	16.0644(10)	12.2719(3)	13.090(3)	13.1063(7)	13.1162(2)
c [Å]	39.878(3)	41.3903(8)	20.798(4)	20.6127(12)	20.5405(2)
α [°]	90	90	98.42(3)	98.198(5)	98.1420(10)
β [°]	102.3020(10)	91.4700(10)	92.87(3)	92.927(3)	93.0010(10)
γ [°]	90	90	101.97(3)	101.795(2)	101.7580(10)
V [Å^3]	25581(3)	4967.62(19)	3275.8(11)	3255.1(3)	3247.45(8)
Z	8	4	2	2	2
ρ_{calcd} [g cm^{-3}]	1.212	1.352	1.222	1.235	1.244
μ [mm^{-1}]	0.856	1.926	0.700	0.845	0.952
reflections collected	49144	37609	35831	43320	46033
unique reflections	24724	10428	14927	14854	14803
parameters varied	1445	595	778	766	755
R(int)	0.0609	0.0680	0.0675	0.1478	0.0501
R_1	0.0704	0.0383	0.0682	0.0873	0.0409
wR_2	0.1506	0.0800	0.1518	0.1218	0.0832

	4Ho	**4Yb**	**5Sm**	**6Ce**	**6Nd**
formula	$C_{71}H_{97}HoN_6O_2$	$C_{71}H_{97}N_6YbO_2$	$C_{82}H_{65}N_6Sm$	$C_{61}H_{86}CeFN_4O$	$C_{54}H_{78}FN_4NdO$
M_r	1231.48	1239.59	1284.75	1050.46	962.44
T [K]	123(2)	123(2)	123(2)	123(2)	123(2)
space group	$P\bar{1}$	$P\bar{1}$	$P\bar{1}$	$P2_1/c$	$P2_1/n$
a [Å]	12.4225(5)	12.406(3)	12.3819(3)	12.10100(10)	10.53490(10)
b [Å]	13.1516(10)	13.125(3)	13.3210(3)	13.87440(10)	27.3368(4)
c [Å]	20.5070(7)	20.598(8)	21.4203(7)	33.8989(4)	18.2547(3)
α [°]	98.590(3)	98.517(10)	100.3250(10)	90	90
β [°]	92.3140(10)	92.409(10)	102.2120(10)	92.7560(10)	102.8970(10)
γ [°]	102.9780(10)	102.535(5)	110.4840(10)	90	90
V [Å^3]	3218.6(3)	3228.3(16)	3108.55(14)	5684.84(9)	5124.55(12)
Z	2	2	2	4	4
ρ_{calcd} [g cm^{-3}]	1.271	1.275	1.373	1.227	1.247
μ [mm^{-1}]	1.278	1.497	0.997	0.846	1.056
reflections collected	22794	18356	34615	39384	33241
unique reflections	11771	10064	15138	13133	12484
parameters varied	755	744	803	630	587
R(int)	0.0840	0.0616	0.0450	0.0675	0.0629
R_1	0.0819	0.0499	0.0534	0.0351	0.0440
wR_2	0.1691	0.1231	0.1121	0.0767	0.0961

	6Nd.tol	**6Tm**	**8**	**9Nd**	**9Sm**
formula	$C_{61}H_{86}FN_4NdO$	$C_{54}H_{78}FN_4OTm$	$C_{35}H_{45}F_3N_2O$	$C_{69}H_{91}N_4NdO$	$C_{69}H_{91}N_4OSm$
M_r	1054.58	987.13	566.73	1136.70	1142.81
T [K]	123(2)	173(2)	123(2)	123(2)	123(1)
space group	$P2_1/c$	$P2_1/n$	$P2_1/n$	$P2_1/c$	$P\bar{1}$
a [Å]	12.1002(2)	20.5998(2)	15.1258(5)	13.8622(3)	12.1196(13)
b [Å]	13.8618(2)	12.1635(2)	14.2672(4)	39.1578(8)	12.4300(16)
c [Å]	33.7996(7)	21.6514(3)	16.3892(5)	12.1555(2)	23.331(3)
α [°]	90	90	90	90	86.785(6)
β [°]	92.8430(10)	110.2870(10)	117.121(2)	109.327(2)	77.789(6)
γ [°]	90	90	90	90	63.880(6)
V [Å^3]	5662.25(17)	5088.56(12)	3147.94(17)	6226.3(2)	3081.6(6)
Z	4	4	4	4	2
ρ_{calcd} [g cm^{-3}]	1.237	1.289	1.196	1.213	1.232
μ [mm^{-1}]	0.962	1.787	0.083	0.878	0.997
reflections collected	36454	30721	38773	32083	52253
unique reflections	13512	11701	7461	13567	14073
parameters varied	630	567	378	694	694
R(int)	0.1365	0.0457	0.1321	0.1087	0.0869
R_1	0.0566	0.0447	0.0619	0.0628	0.0948
wR_2	0.1017	0.1163	0.1316	0.1102	0.2274

[a] Cell parameters for **3Sm** for reference: $T = 123$ K; $a = 41.310(8)$, $b = 16.257(3)$, $c = 39.920(8)$ Å, $\beta = 103.01(3)°$, V = 26122(9) Å^3.

are included in Table 2 for reference. The data collected for this compound were incomplete and of poor quality due to suspected twinning. The similarity of unit cell data (Table 2) and connectivity of the refined [Ln(Form)$_3$] units of **3Sm** suggest that it is most likely isomorphous with **3Nd**.

Lanthanoid o-TolForm complexes: Compound **1La** crystallises in the tetragonal, space group $I4_1/acd$ with half of the molecule comprising the asymmetric unit. The [La(*o*-TolForm)$_3$(thf)$_2$] molecular unit exhibits two *transoid* THF donor molecules (Figure 1, top), giving the eight-coordinate lanthanum metal centre a compressed trigonal prismatic LaN_6 geometry with two trigonal-face-capping THF oxygen atoms (Figure 1, bottom: O(1)-La(1)-O(1)# 157.23(17)°). The average La–N and La–O bond lengths are 2.62 and 2.60 Å respectively. There are no crystallographically characterised lanthanoid *o*-TolForm complexes with which to compare **1La** but the La–N bond lengths are similar to those of [{O(SiMe$_2$-Ap)$_2$}$_2$LaRh(cod)] (Ap = 2-amino-4-methylpyridinate, cod = cycloocta-1,5-diene; av La–N bond length 2.64 Å).[27]

Compound **1Yb** crystallises in the triclinic space group $P\bar{1}$ with one molecule comprising the asymmetric unit. The seven-coordinate ytterbium centre has three chelating *N,N′*-bis(aryl)formamidinate ligands and one THF molecule (Figure 2, top left). The decrease in coordination number from **1La** is consistent with the decrease in ionic radius (0.16 Å) of Yb^{3+} relative to La^{3+}.[28] The related compound **1YbOH** crystallises in the monoclinic space group $P2_1/c$ with half of the molecule comprising the asymmetric unit. This dinuclear species (Figure 2, top right) consists of two seven-coordinate Yb^{3+} metal centres that are bridged by two hydroxyl groups. Each Yb^{3+} metal centre is bound by two chelating *o*-TolForm ligands and a single THF molecule. The two Yb^{3+} atoms and two bridging oxygen atoms are coplanar with the sum of the angles within the Yb_2O_2 metallacycle amounting to 360.0(4)°. The geometries about the Yb^{3+} centres of **1Yb** and **1YbOH** are best described as a distorted pentagonal bipyramid (Figure 2, bottom left) and a distorted N(2) face-capped triangular prism (Figure 2, bottom right) respectively. The distorted pentagonal bipyramid of **1Yb** is composed of the apical N(6) and O(1) atoms and the remaining five

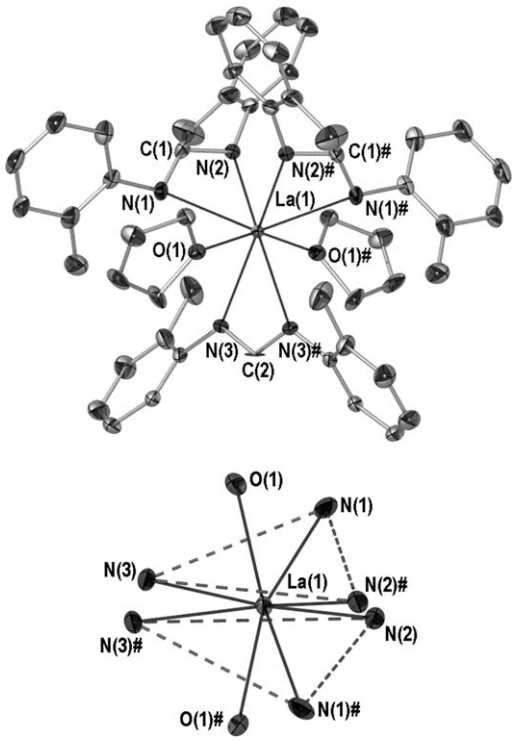

Figure 1. Top: Molecular structure of **1La**. All hydrogen atoms and lattice solvent omitted for clarity. Symmetry transformation used to generate '#' atoms: $^1/_2$-x, y, $-z$. Bottom: Central coordination polyhedron of **1La** depicting flattened bicapped LaN_6O_2 trigonal prism.

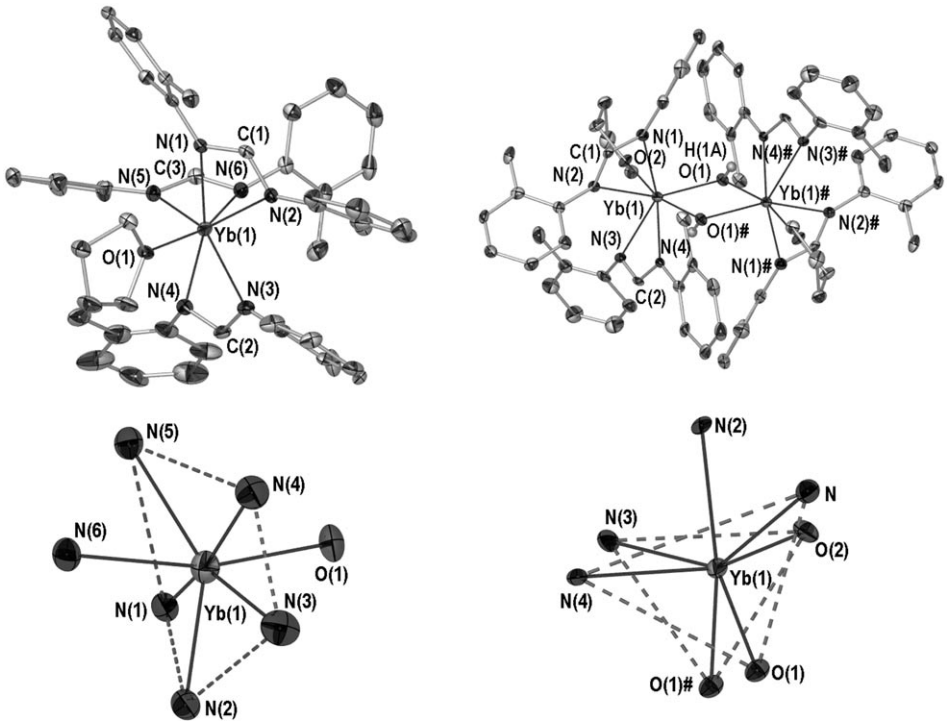

Figure 2. Top left: Molecular structure of [Yb(*o*-TolForm)$_3$(thf)] (**1Yb**). All hydrogen atoms omitted for clarity. Bottom left: Yb coordination polyhedron. Top right: Molecular structure of [{Yb(*o*-TolForm)$_2$(μ-OH)(thf)}$_2$] (**1YbOH**). All hydrogen atoms and lattice solvent omitted for clarity. Symmetry transformation used to generate "#" atoms: $1-x$, $2-y$, $1-z$. Bottom right: Yb coordination polyhedron. Selected bond lengths (Å) and angles (°) not listed in Table 3: Yb(1)–O(1)# 2.232(6), O(1)-Yb(1)-O(1)# 67.9(2), Yb(1)-O(1)-Yb(1)# 112.1(2).

nitrogen atoms in the equatorial positions (Figure 2, bottom left). The apical atoms O(1) and N(6) approach a linear arrangement across ytterbium (161.47(17)°), but cannot be fully linear due to the metal chelated nature of the N(5)-C(3)-N(6) unit. In **1YbOH**, the two triangular faces of the capped triangular prism are distorted due to constraints imposed by the NCN backbone angles of one *o*-TolForm ligand, the bridging Yb(μ-OH)$_2$Yb unit and the N···N distances (Figure 2, bottom left).

The Yb–N bond lengths in **1Yb** and **1YbOH** are comparable (2.343(5) to 2.410(5) Å in **1Yb** and 2.378(6) to 2.420(6) Å in **1YbOH**); they also exhibit comparable Yb–O_{thf} bond lengths (**1Yb** 2.336(4) Å; **1YbOH** 2.358(6) Å). The Yb–$O_{hydroxyl}$ bond lengths in **1YbOH** are 2.202(6) and 2.232(6) Å, which are shorter than the Yb–$O_{hydroxyl}$ bond lengths found in [{Yb(Cp′)$_2$(μ-OH)}$_2$] (Cp′ = $C_5H_4SiMe_3$; 2.25(2) to 2.33(2) Å),[29] and within the range provided by the five-coordinate [{Yb(OC$_6$H$_3$-2,6-*t*Bu$_2$)$_2$(μ-OH)(thf)}$_2$] complex (2.196(6) to 2.38(8) Å).[30]

Lanthanoid XylForm and MesForm complexes: In compound **2La** (triclinic space group $P\bar{1}$ with one molecule in the asymmetric unit) the lanthanum metal centre is seven-coordinate and bound by three chelating XylForm ligands and one THF ligand (Figure 3). Its geometry can be described as a face-capped trigonal prism (Figure 3, bottom). The La–N bond lengths in **2La** range from 2.5610(15) to 2.6173(14) Å and the La–O bond length 2.5760(12) Å is comparable with the mean distance of **1La** (2.600(4) Å) allowing for ionic radii differences (CN = 7; ionic radius = 1.10 Å, CN = 8; ionic radius = 1.16 Å).[28] Similarly, the La–O bond length in **2La** is shorter than that in [{O(SiMe$_2$-Ap)$_2$}$_2$LaRh(cod)] (mean 2.64 Å)[27] and surprisingly comparable with the five-coordinate [La(DippBenz)(CH$_2$Ph)$_2$(thf)] (DippBenz = *N,N′*-bis-(2,6-diisopropylphenyl)benzamidinate) complex, which has a La–O_{thf} bond length of 2.557(3) Å.[31]

The use of a smaller lanthanoid, such as samarium (CN = 6; ionic radii Sm = 0.95 Å; La = 1.03 Å) gives the six-coordinate homoleptic complex **2Sm** (Figure 4). Complex **2Sm** crystallises in the monoclinic space group $P2_1$ with two molecules in the asymmetric unit. Both unique molecules possess similar metric parameters and only that of Sm(1) is discussed here and listed in Table 3 (see Scheme 2 for reference key). The samarium geometry in **2Sm** can be described as a distorted trigonal prism (Figure 4, bottom) similar to the LaN_6 array of **2La** with the three NCN chelates straddling the trigonal planes.

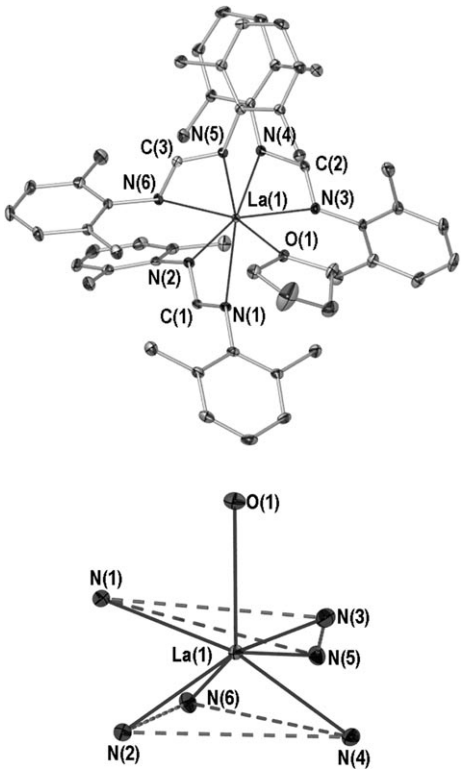

Figure 3. Top: Molecular structure of [La(XylForm)$_3$(thf)] (**2La**). All hydrogen atoms and lattice solvent omitted for clarity. Bottom: Lanthanum coordination polyhedron.

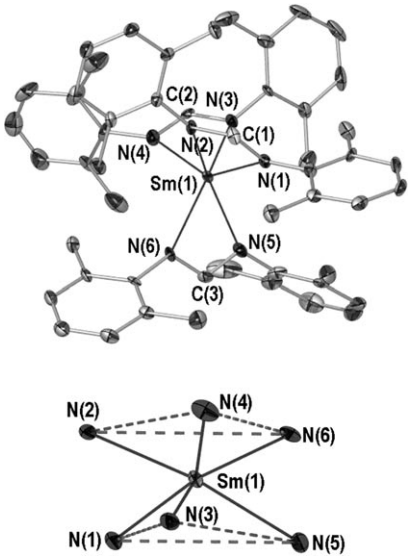

Figure 4. Top: Molecular structure of [Sm(XylForm)$_3$] (**2Sm**). All hydrogen atoms omitted for clarity. Bottom: Samarium coordination polyhedron.

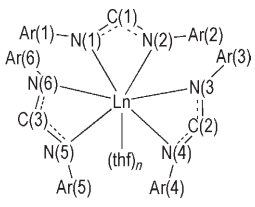

Scheme 2. Reference key for Table 3.

Compounds **3Nd**, **3Sm** and **3Yb** are homoleptic six-coordinate complexes and are isostructural with **2Sm**. Compounds **3Nd** and **3Sm** are isomorphous and crystallise in the monoclinic space group *C*2/*c* with two near identical complete [Ln(MesForm)$_3$] molecules in the asymmetric unit. The poor quality of the data collect-

Table 3. Selected bond lengths [Å] and angles [°] for **1Ln–5Ln** complexes. See reference key (Scheme 2) and/or relevant figure for atomic reference.

	1La[a]	**1Yb**	**1YbOH**[b]	**2La**	**2Sm**[c]	**3Nd**[c]	**3Yb**
Ln(1)–N(1)	2.632(5)	2.410(5)	2.420(6)	2.5610(15)	2.447(7)	2.477(5)	2.348(3)
Ln(1)–N(2)	2.602(4)	2.365(5)	2.406(7)	2.5955(14)	2.425(7)	2.440(5)	2.375(3)
Ln(1)–N(3)	2.623(4)	2.344(5)	2.400(6)	2.5611(14)	2.431(7)	2.452(5)	2.349(3)
Ln(1)–N(4)	2.623(4)	2.395(5)	2.378(6)	2.5681(14)	2.455(8)	2.486(6)	2.354(3)
Ln(1)–N(5)	2.602(4)	2.398(5)	-	2.5901(14)	2.421(7)	2.464(7)	2.348(3)
Ln(1)–N(6)	2.632(5)	2.343(5)	-	2.6173(14)	2.438(7)	2.460(7)	2.329(3)
Ln(1)–O(1)	2.600(4)	2.336(4)	2.202(6)	2.5760(12)	–	–	–
Ln(1)–O(2)	2.600(4)	–	2.358(6)	–	–	–	–
C(1)–N(1)	1.316(7)	1.310(8)	1.339(10)	1.319(2)	1.306(12)	1.319(8)	1.322(4)
C(1)–N(2)	1.318(7)	1.319(8)	1.300(8)	1.324(2)	1.328(12)	1.320(8)	1.329(4)
C(2)–N(3)	1.325(5)	1.303(9)	1.330(10)	1.324(2)	1.299(11)	1.334(9)	1.332(4)
C(2)–N(4)	1.325(5)	1.334(9)	1.313(9)	1.325(2)	1.292(12)	1.321(8)	1.321(4)
C(3)–N(5)	1.318(7)	1.327(8)	-	1.324(2)	1.331(12)	1.327(11)	1.318(4)
C(3)–N(6)	1.316(7)	1.304(8)	-	1.323(2)	1.348(12)	1.328(10)	1.315(4)
N(1)-Ln(1)-N(2)	51.97(14)	56.20(17)	56.7(2)	52.62(4)	55.3(2)	55.05(16)	57.55(9)
N(1)-C(1)-N(2)	121.1(5)	117.6(6)	117.8(7)	119.71(15)	118.2(8)	118.9(6)	118.1(3)
N(3)-Ln(1)-N(4)	51.55(18)	56.8(2)	55.8(2)	52.90(5)	55.2(3)	54.92(18)	58.37(10)
N(3)-C(2)-N(4)	118.9(6)	117.5(6)	118.4(7)	119.20(15)	121.9(8)	118.1(6)	119.6(3)
N(5)-Ln(1)-N(6)	51.97(14)	57.35(18)	-	52.42(4)	56.2(3)	54.8(2)	57.92(10)
N(5)-C(3)-N(6)	121.1(5)	119.7(6)	-	120.65(16)	117.5(8)	117.0(9)	118.6(3)
Ar(1):LnNCN	51.6(6)	48.1(3)	38.1(6)	73.5(2)	58.1(7)	82.0(3)	87.8(1)
Ar(2):LnNCN	70.1(4)	57.8(3)	80.4(5)	67.9(2)	52.9(6)	21.9(5)	7.8(3)
Ar(3):LnNCN	42.7(2)	46.0(6)	54.4(5)	62.7(6)	62.1(7)	75.9(7)	51.6(3)
Ar(4):LnNCN	42.7(2)	50.5(6)	14.9(5)	73.1(1)	83.3(7)	75.5(7)	89.0(2)
Ar(5):LnNCN	70.1(4)	40.2(5)	-	56.7(2)	84.4(7)	87.6(3)	68.0(2)
Ar(6):LnNCN	51.6(6)	65.9(5)	-	88.9(1)	64.1(6)	79.3(8)	85.1(2)
trigonal faces	[d]	na	N(1)N(4)O(1): O(2)N(3)O(1)#	[d]	[d]	[d]	[d]
torsion of prism[e]	39.5(6)	na	27.1(8)	32.5(9)	23.9(9)	14.9(8)	14.2(9)

	4La	**4Nd**	**4Sm**	**4Ho**	**4Yb**	**5Sm**
Ln(1)–N(1)	2.522(4)	2.459(5)	2.442(2)	2.379(8)	2.344(4)	2.418(3)
Ln(1)–N(2)	2.523(4)	2.468(4)	2.444(2)	2.386(7)	2.352(5)	2.452(3)
Ln(1)–N(3)	2.530(4)	2.477(4)	2.451(2)	2.386(7)	2.354(5)	2.427(3)
Ln(1)–N(4)	2.539(4)	2.480(4)	2.442(2)	2.377(7)	2.339(5)	2.463(3)
Ln(1)–N(5)	2.516(4)	2.462(4)	2.442(2)	2.367(6)	2.341(5)	2.491(3)
Ln(1)–N(6)	2.515(4)	2.451(5)	2.427(2)	2.379(7)	2.328(4)	2.425(3)
C(1)–N(1)	1.329(6)	1.327(7)	1.326(4)	1.330(12)	1.315(8)	1.333(5)
C(1)–N(2)	1.318(7)	1.316(7)	1.316(4)	1.327(13)	1.323(7)	1.317(5)
C(2)–N(3)	1.317(6)	1.316(6)	1.324(3)	1.349(12)	1.338(7)	1.315(5)
C(2)–N(4)	1.317(6)	1.319(6)	1.320(4)	1.292(12)	1.310(7)	1.324(5)
C(3)–N(5)	1.316(6)	1.324(6)	1.327(4)	1.308(12)	1.321(6)	1.327(5)
C(3)–N(6)	1.326(6)	1.314(6)	1.326(3)	1.329(11)	1.334(7)	1.318(5)
N(1)-Ln(1)-N(2)	53.98(14)	55.09(15)	55.64(8)	57.0(3)	57.65(16)	55.11(11)
N(1)-C(1)-N(2)	119.8(4)	119.0(5)	119.3(3)	117.6(9)	118.3(5)	116.5(3)
N(3)-Ln(1)-N(4)	53.35(13)	54.80(14)	55.44(7)	56.4(3)	57.78(16)	54.79(11)
N(3)-C(2)-N(4)	119.5(4)	119.9(5)	118.7(2)	116.9(8)	117.8(5)	117.0(3)
N(5)-Ln(1)-N(6)	54.19(13)	55.49(14)	56.17(7)	57.4(3)	58.33(15)	54.92(10)
N(5)-C(3)-N(6)	120.3(4)	120.3(5)	119.6(3)	119.5(8)	118.0(5)	118.1(3)
Ar(1):LnNCN	69.8(5)	68.0(5)	67.3(3)	65.8(8)	67.3(6)	33.9(5)
Ar(2):LnNCN	61.6(4)	61.8(4)	62.2(2)	63.3(6)	61.0(4)	37.4(4)
Ar(3):LnNCN	58.9(5)	60.1(5)	60.4(3)	62.7(9)	60.5(4)	49.3(4)
Ar(4):LnNCN	65.4(4)	66.3(4)	67.5(2)	65.3(7)	67.6(4)	41.2(3)
Ar(5):LnNCN	64.8(3)	64.3(4)	64.4(2)	64.4(6)	66.3(4)	46.5(3)
Ar(6):LnNCN	75.4(4)	75.2(5)	76.0(2)	78.0(8)	75.6(5)	48.0(3)
trigonal faces	[d]	[d]	[d]	[d]	[d]	[d]
torsion of prism[e]	19.5(2)	21.5(2)	22.6(1)	23.6(3)	25.9(2)	20.6(10)

[a] N(4)=N(3)#, N(5)=N(2)#, N(6)=N(1)#, O(2)=O(1)#, Ar(4)=Ar(3)#, Ar(5)=A(2)#, Ar(6)=Ar(1)#. Symmetry transformation used to generate "#" atoms: $^1/_2-x$, y, $-z$. [b] Symmetry transformation used to generate "#" atoms: $1-x$, $2-y$, $1-z$. [c] Where two molecular units present in asymmetric unit, bond lengths and angles provided for lowest numbered molecule. [d] Trigonal prism composed of N(1)N(3)N(5) and N(2)N(4)N(6) trigonal faces. [e] Torsion calculated using torsional angle of Ln(1)N(1)centroid:Ln(1)N(2)centroid, in which centroid refers to centroid of trigonal face containing either N(1) or N(2).

ed for the latter prohibit further discussion of its bond lengths and angles. Complex **3Yb** crystallises in the monoclinic space group $P2_1/n$ with one complete molecule in the asymmetric unit. A noteworthy trend for the trigonal pris-

matic LnN_6 geometries of **2La**, **2Sm**, **3Nd** and **3Yb** is the decreasing twist[32] of the triangular planes relative to one another; torsion angle **2La** 32.5(9)°; **2Sm** 23.9(9)°; **3Nd** 14.9(8)°; **3Yb** 14.2(9)°. Although THF-coordinated **2La** is not directly comparable, the observed decrease in twist occurs with an increase in mean N-Ln-N chelate angle across the lanthanoid series (**2La** 52.7°; **2Sm** 55.6°; **3Nd** 54.9°; **3Yb** 58.0°) and no consistent modification of ligand N-C-N angle (mean **2La** 119.9°; **2Sm** 119.2°; **3Nd** 118.0°; **3Yb** 118.8°). Accordingly, the contraction in Ln–N bond length (av Ln–N bond length: seven-coordinate La–N 2.582 Å; six-coordinate Nd–N 2.463 Å; Sm–N 2.436 Å; Yb–N 2.351 Å) and opening of the chelate bite results in diminished twisting of the trigonal planes relative to one another.

Lanthanoid EtForm and PhPhForm complexes: The homoleptic compounds **4La**, **4Nd**, **4Sm**, **4Ho** and **4Yb** are isomorphous and crystallise in the triclinic space group $P\bar{1}$ (**4Ho**; Figure 5). Like **2Sm**, **3Nd** and **3Yb**, the **4Ln** compounds are trigonal prismatic. However, in contrast to the **2Ln** and **3Ln** complexes, the twisting of the two triangular faces increases with decreasing Ln ionic radius: **4La** 19.5(2)°; **4Nd** 21.5(2)°; **4Sm** 22.6(1)°; **4Ho** 23.6(1)°; **4Yb** 25.9(2)°. There is a gradual increase in mean N-Ln-N chelate angle (**4La** 53.8°; **4Nd** 55.1°; **4Sm** 55.8°; **4Ho** 56.9°; **4Yb** 57.9)° with decreasing metallic radius, as per **2Ln** and **3Ln** complexes; however, this occurs in conjunction with a decrease in mean ligand N-C-N angle across the *N,N′*-chelating EtForm (**4La** 119.9°; **4Nd** 119.7°; **4Sm** 119.2°; **4Ho** 118.0°; **4Yb** 118.0°). Thus, as the mean N-Ln-N bites and Ln–N bond lengths are comparable for **2Ln**, **3Ln** and **4Ln** species with similar metallic radii (**4Ln** Ln–N bond lengths; La–N 2.52 Å; Nd–N 2.47 Å; Sm–N 2.44 Å; Ho–N 2.38 Å; Yb–N 2.34 Å), and the five **4Ln** species are isomorphous, the increase in twist about the triangular prism must be facilitated by opening of the *N,N′*-chelate donor set of EtForm.

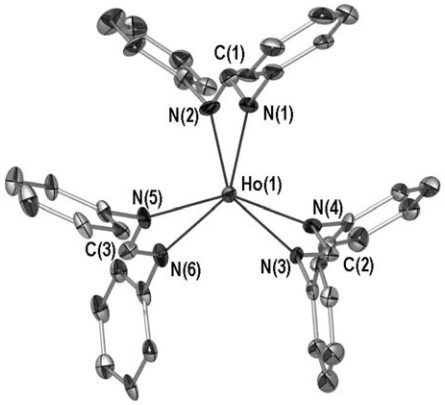

Figure 5. Molecular structure of [Ho(EtForm)$_3$] (**4Ho**). Aryl ethyl substituents, hydrogen atoms and lattice solvent omitted for clarity.

The average Nd–N bond length in **3Nd** (2.46 Å) and **4Nd** can be compared with the Nd–N bond lengths found in the closely related homoleptic complex [Nd(CyNC(Me)NCy)$_3$] (2.445(3) to 2.473(2) Å).[33] The only crystallographically authenticated ytterbium homoleptic tris(amidinate) complexes are [Yb(CyNC(Me)NCy)$_3$] and [Yb(CyNC(Ph)NCy)$_3$],[5a] for which the Yb–N bond lengths range from 2.300(8) to 2.361(7) Å and 2.321(5) to 2.333(5) Å, respectively. These compare reasonably well with the bond lengths found in **3Yb** and **4Yb**.

Compound **5Sm** (Figure 6) crystallises in the triclinic space group $P\bar{1}$ with one molecule in the asymmetric unit. The homoleptic [Sm(*o*-PhPhForm)$_3$] unit exhibits three chelating amidinate ligands and a single η^1-π-arene bonding interaction from a pendant *ortho*-phenyl ring (Sm(1)–C(11) 3.017(5) Å), giving overall seven-coordination. This interaction is in accord with bonding parameters for the η^6-Ph–Sm interaction of [{Sm(OC$_6$H$_3$-2,6-*i*Pr$_2$)$_3$}$_2$], for which Sm–C contacts range from 2.824(7) to 3.160(8) Å,[34] and in accordance with intramolecular Nd–π-arene contacts observed for [Nd(OC$_6$H$_3$-2,6-Ph$_2$)$_3$] (2.946(6)–3.258(9) Å) and [Nd(OC$_6$H$_3$-2,6-Ph$_2$)$_3$(thf)] (3.010(5)–3.144(5) Å)[35] with coordination number and lanthanoid radii taken into consideration.[28] Beyond Sm(1)–C(11), the shortest Sm···C distance is that of Sm(1)···C(12) (3.474(5) Å), which is too long to be considered a samarium–carbon interaction. The Sm–N bond lengths in **5Sm** range from 2.418(3) to 2.491(3) Å and are comparable with the Sm–N bond lengths found in **2Sm** (av 2.436 Å) and **4Sm** (see above and Table 3), despite the additional Sm–C interaction in **5Sm**, a feature sought in choice of this ligand.

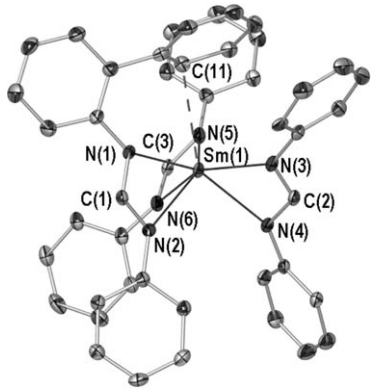

Figure 6. Molecular structure of [Sm(PhPhForm)$_3$] (**5Sm**). All hydrogen atoms, non-coordinating *o*-phenyl groups and lattice solvent omitted for clarity. Selected bond lengths (Å) and torsion angles (°) not listed in Table 3: Sm(1)–C(11) 3.017(5), non-bonding Sm(1)···C(12) 3.474(5), Ar(1):Sm(1)N(1)C(1)N(2) 33.9(5).

Comparison of [Ln(Form)$_3$(thf)$_n$] complexes: The *o*-TolForm ligand gives an eight-coordinate La complex (**1La**) and a seven-coordinate Yb complex (**1Yb**). On the basis of empir-

ical composition, **1Er** may have a similar structure to **1Yb**. Replacement of the *ortho*-methyl of *o*-TolForm with a phenyl (*o*-PhPhForm), as per **5Sm**, results in seven-coordination with a single η^1-Ph–Sm interaction supplementing SmN_6 ligation. Thus, it would clearly be of interest to also have molecular structures of [Ln(*o*-PhPhForm)$_3$] complexes from nearer the ionic radius extremities to monitor the effect of metal size on metal–arene interactions. Addition of a second *ortho*-methyl substituent (XylForm) gives a seven-coordinate lanthanum complex (**2La**) and a six-coordinate samarium complex (**2Sm**). The MesForm ligand, with its additional *para*-methyl substituent, forms six-coordinate lanthanoid complexes with Nd (**3Nd**), Sm (**3Sm**) and Yb (**3Yb**). Since we could not obtain a structure for **3La**, a higher coordination number than six for **3La** cannot be excluded. Indeed, the composition of **2La** suggests **3La** is most likely [La(MesForm)$_3$(thf)]·THF based on the analytical data available.

As per the structurally characterised **3Ln** complexes, the larger ethyl substituents of EtForm fail to induce structural variation across the **4Ln** lanthanoid series. Thus, the EtForm ligand is sufficiently bulky to limit coordination to a maximum of six with the larger Ln metals, but cannot impede the final ligand exchange [Eq. (3)] and thereby induce C–F activation of a coordinated perfluoroaryl [Eq. (4)] for the smaller Ln metals.

The N-Ln-N bite angles of the *N,N′*-bis(aryl)formamidinate ligands appear to be affected by the addition of a CH_3 group in the *ortho*-phenyl position of *o*-TolForm to give XylForm. This can be seen for the lanthanum structures: **1La**: 51.55(18)° to 51.97(14)°; **2La**: 52.42(4)° to 52.90(5)°. Replacement of the *o*-methyl with a *o*-phenyl to give *o*-PhPhForm group causes less increase in the N-Ln-N bite angle of the *N,N′*-bis(aryl)formamidinate ligands than two *ortho*-substituents, as demonstrated by **2Sm** (55.2(3)–56.2(3)°), **4Sm** (55.44(7)–56.17(7)°) and **5Sm** (54.79(11)–55.11(11)°). Following the same trend, the interplanar angles of the arene rings with respect to the M-N-C-N metallacycle plane are significantly affected across the three lanthanum complexes (**1La** 42.7(2)–70.1(4)°; **2La** 56.7(2)–88.9(1)°; **4La** 58.9(5)–75.4(4)°). Compound **1La** displays the smallest arene twisting out of the M-N-C-N plane, while seven-coordinate XylForm complex **2La** exhibits greater twisting than six-coordinate **4La**, due to enhanced spatial congestion in **2La**. Complexes of ytterbium show a similar trend with increased torsion across the ligand series induced by shorter Ln–N distances and increased steric crowding (2.376 Å **1Yb**; 2.401° **1YbOH**; 2.351 **3Yb**; 2.343 **4Yb**). Where available, comparison of the bonding in **6Ln** species with [Ln(Form)$_3$(thf)$_n$] complexes containing smaller *N,N′*-bis(aryl)formamidinate ligands reveals no consistent pattern in bond lengths aside from the established correlation with coordination number. For instance, the lanthanum complexes exhibit average La–N bond lengths of **1La** 2.62 Å, **2La** 2.58 Å, **4La** 2.52 Å, and **6La** 2.55 Å, which suggests an expected decrease in bond lengths with decreasing coordination number, and an increase in bond lengths with increased *N,N′*-bis(aryl)formamidinate steric bulk when six-coordinate complexes are compared (**4La** and **6La**).

In summary, *o*-TolForm exhibits the greatest structural variety, while the XylForm, MesForm, EtForm and *o*-PhPhForm ligands restrain the lanthanoid metal centre resulting in homoleptic complexes for the last three ligands. The structure of **5Sm** shows that intramolecular π-Ar–Ln binding (η^1) is possible with *N,N′*-bis(2-biphenylyl)formamidinates.

[Ln(DippForm)$_2$F(thf)] complexes: Compounds **6La**,[10] **6Ce**, **6Nd** (both as toluene and non-toluene solvate), **6Sm**[8] and **6Tm** are isostructural despite crystallizing in several different crystal systems (Table 2). Compounds **6La** and **6Ce** crystallise with a single lattice toluene molecule, while **6Sm** and **6Tm** are lattice solvent-free. Compound **6Nd** crystallises as both the toluene solvate (isomorphous with **6Ce**) and the non-solvate (isomorphous with **6Sm** and **6Tm**) from toluene. The molecular structures of all **6Ln** compounds are six-coordinate with *cisoid* fluoride and THF ligands. Akin to lanthanoid complexes of the smaller *N,N′*-bis(aryl)formamidinates, the geometry about the lanthanoid centres of the **6Ln** species can be described as a trigonal prism with trigonal faces composed of N(1)F(1)N(4):N(2)O(1)N(3) (**6Ce**; Figure 7, Table 4, Scheme 3). These mononuclear [LnL$_2$F] complexes boast not only a rare terminal fluoride,[8,10,12c,13c,36] but are also the first lanthanoid fluorides supported by organoamide ligands. Comparison with the few terminal Ln–F complexes indicates similar metric parameters, for example, higher coordinate [Sm(Tp*)$_2$(F)] (Sm–F 2.089(3) Å; **6Sm** 2.093(2) Å),[8,36] and [Ce(1,2,4-*t*Bu$_3$C$_5$H$_2$)$_2$F] (Ce–F 2.165(4) Å,[13c] **6Ce** 2.1217(15) Å). The Ln(1)–F(1) bonding of the

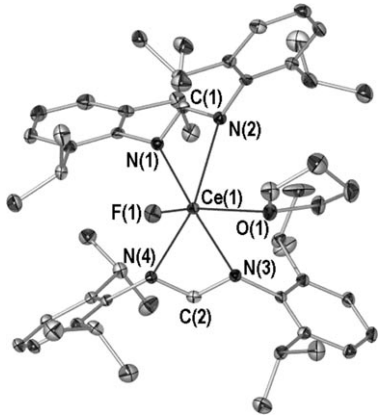

Figure 7. Molecular structure of [Ce(DippForm)$_2$F(thf)] (**6Ce**). All hydrogen atoms and lattice solvent omitted for clarity.

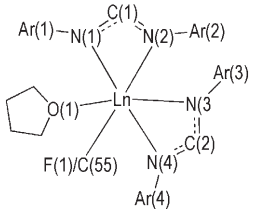

Scheme 3. Reference key for Table 4.

Table 4. Selected bond lengths [Å] and angles [°] for **6Ln** complexes including **6La**[10] and **6Sm.**[8] See reference key (Scheme 3) and/or relevant figure for atomic reference.

	6La[10]	**6Ce**	**6Nd·tol**	**6Nd**	**6Sm**[8]	**6Tm**
Ln(1)–N(1)	2.538(3)	2.4893(19)	2.449(4)	2.456(2)	2.443(3)	2.345(3)
Ln(1)–N(2)	2.578(3)	2.556(2)	2.530(4)	2.501(3)	2.454(3)	2.364(3)
Ln(1)–N(3)	2.543(3)	2.512(2)	2.484(4)	2.459(3)	2.446(3)	2.365(3)
Ln(1)–N(4)	2.560(3)	2.547(2)	2.515(4)	2.490(3)	2.454(3)	2.361(3)
Ln(1)–O(1)	2.539(3)	2.5099(16)	2.476(3)	2.490(3)	2.457(2)	2.359(3)
Ln(1)–F(1)	2.136(2)	2.1217(15)	2.100(3)	2.128(2)	2.093(2)	2.020(2)
C(1)–N(1)	1.319(4)	1.324(3)	1.327(5)	1.347(4)	1.320(4)	1.331(5)
C(1)–N(2)	1.316(5)	1.322(3)	1.327(5)	1.319(4)	1.340(4)	1.317(5)
C(2)–N(3)	1.322(4)	1.321(3)	1.332(5)	1.315(4)	1.332(4)	1.328(5)
C(2)–N(4)	1.316(4)	1.325(3)	1.317(5)	1.323(4)	1.321(4)	1.325(5)
N(1)-Ln(1)-N(2)	53.02(9)	53.63(6)	54.50(11)	55.00(8)	55.55(9)	57.62(10)
N(1)-C(1)-N(2)	120.1(3)	118.7(2)	118.9(4)	118.3(3)	118.1(3)	117.9(3)
N(3)-Ln(1)-N(4)	53.04(9)	53.77(6)	54.40(12)	54.65(8)	55.75(8)	57.57(10)
N(3)-C(2)-N(4)	119.4(3)	119.7(2)	119.2(4)	118.9(3)	119.5(3)	118.2(3)
O(1)-Ln(1)-F(1)	85.1(1)	87.02(6)	86.54(10)	80.07(11)	82.16(8)	82.58(9)
Ar(1):LnNCN	81.3(3)	64.8(2)	67.9(2)	64.9(3)	66.8(3)	65.7(3)
Ar(2):LnNCN	74.1(3)	87.0(2)	83.8(2)	86.0(3)	79.5(3)	75.2(2)
Ar(3):LnNCN	88.2(3)	87.8(2)	82.5(3)	87.3(3)	59.2(2)	78.3(3)
Ar(4):LnNCN	80.7(2)	71.6(2)	88.4(2)	71.6(3)	73.2(1)	66.2(3)
trigonal faces	N(1)F(1)N(4): N(3)O(1)N(2)	N(1)F(1)N(4): N(3)O(1)N(2)	N(1)F(1)N(4): N(3)O(1)N(2)	N(1)F(1)N(4): N(3)O(1)N(2)	N(1)F(1)N(4): N(3)O(1)N(2)	N(1)F(1)N(4): N(3)O(1)N(2)
torsion of prism[a]	30.2(5)	33.5(3)	32.6(3)	28.9(6)	17.9(5)	31.3(3)

[a] Torsion calculated using torsional angle of Ln(1)N(1)centroid:Ln(1)N(2)centroid, in which centroid refers to centroid of trigonal face containing either N(1) or N(2).

6Ln complexes is consistent with a reduction in lanthanoid radius across the series (Table 4).

[Ln(DippForm)$_2$(C≡CPh)(thf)] complexes: The molecular structures of the phenylethynyl compounds **9Nd** (Figure 8) and **9Sm** are consistent with bonding parameters found for **6Nd** and **6Sm** respectively (see Tables 4 and 5 and Figure 8 caption). The coordination environment about the neodymium and samarium centres is near identical once ionic radii differences are taken into account.[28] The main distinguishing feature between the two structures is the Ln-C(55)-C(56) angle of the phenylethynyl link. In **9Nd**, the angle is close to linear (170.9(4)°, Nd–C(55) 2.451(5) Å), while in **9Sm** the corresponding angle is 142.9(7)° (Sm–C(55) 2.398(9) Å). This deviation from linearity for **9Sm** has little impact on the C≡C bond length relative to that of **9Nd** (**9Nd**; 1.227(7) Å, **9Sm**; (1.214(13) Å). As for the fluoro **6Ln** complexes, the coordination geometry about the LnN_4CO polyhedron is best considered a trigonal prism with trigonal faces composed of N(1)C(55)N(4) and N(3)O(1)N(4). The nominal torsion about these trigonal planes indicates no increased strain within **9Sm** relative to **9Nd** (**9Nd**; 31.5(2)°, **9Sm**; 31.4(7)°), perhaps due to skewing of the CCPh group to alleviate congestion resulting from the decreased Ln–N bond lengths of the former (av **9Sm**; 2.44 Å, **9Nd**; 2.47 Å). The Ln(1)–C(55) distances are comparable with those of other lanthanoid complexes with rare terminal Ln(C≡CR) bonding[9,24c] when ionic radii and coordination number differences are considered, for example, five-coordinate [Er(OC$_6$H$_2$-2,6-*t*Bu$_2$-4-OMe)$_2$(CCPh)(thf)$_2$] (Er–C_{CCPh} 2.31(1) Å)[9] and eight-coordinate [SmCp*$_2$-(CCPh)(thf)] (Sm–C_{CCPh} 2.50(1) Å).[24c]

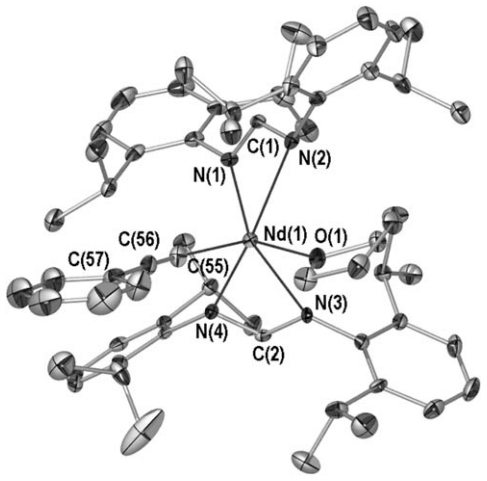

Figure 8. Molecular structure of [Nd(DippForm)$_2$(CCPh)(thf)] (**9Nd**). All hydrogen atoms and lattice solvent omitted for clarity. Selected bond lengths (Å) and angles (°) not listed in Table 5 (**9Sm** parameters in parentheses): C(55)–C(56) 1.227(7) (1.214(13)), C(56)–C(57) 1.451(7) (1.441(13)), Nd(1)-C(55)-C(56) 170.9(4) (142.9(7)), C(55)-C(56)-C(57) 178.3(6) (174.9(10)).

N,N′-*Bis(2,6-diisopropylphenyl)*-N-*{4-(3′,4′,5′-trifluorophenoxy)butyl}formamidine (**8**)*: During preparation of **6La**, **6Nd** and **6Sm** using bis(2,3,4,5-tetrafluorophenyl)mercury (Hg(*o*-$C_6F_4H)_2$ analogue of equation 8), the functionalised *N,N′*-bis(aryl)formamidine co-product **8** was isolated as a colourless crystalline compound. The molecular structure of compound **8** is displayed in Figure 9 (POV-RAY illustration, 40% thermal ellipsoids). Compound **8** exhibits a DippForm

Table 5. Selected bond lengths [Å] and angles [°] for **9Ln** complexes. See reference key in Table 4 and/or relevant figure for atomic reference.

	9Nd	**9Sm**
Ln(1)–N(1)	2.444(4)	2.434(5)
Ln(1)–N(2)	2.515(4)	2.444(6)
Ln(1)–N(3)	2.439(4)	2.418(6)
Ln(1)–N(4)	2.498(4)	2.473(6)
Ln(1)–O(1)	2.474(3)	2.474(5)
Ln(1)–C(55)	2.451(5)	2.398(9)
C(1)–N(1)	1.327(5)	1.330(8)
C(1)–N(2)	1.314(5)	1.319(9)
C(2)–N(3)	1.324(5)	1.310(9)
C(2)–N(4)	1.322(5)	1.304(9)
N(1)-Ln(1)-N(2)	54.59(12)	55.52(18)
N(1)-C(1)-N(2)	119.0(4)	118.1(6)
N(3)-Ln(1)-N(4)	55.08(11)	55.3(2)
N(3)-C(2)-N(4)	119.4(4)	120.7(7)
O(1)-Ln(1)-C(55)	81.72(14)	83.7(3)
Ar(1):LnNCN	60.1(3)	67.6(5)
Ar(2):LnNCN	81.9(4)	71.7(4)
Ar(3):LnNCN	88.1(3)	82.7(5)
Ar(4):LnNCN	70.8(3)	84.8(4)
trigonal faces	N(1)C(55)(N4): N(3)O(1)N(4)	N(1)C(55)(N4): N(3)O(1)N(4)
torsion of prism[a]	31.5(2)	31.4(7)

[a] Torsion calculated using torsional angle of Ln(1)N(1)centroid:Ln(1)N(2)centroid, in which centroid refers to centroid of trigonal face containing either N(1) or N(2).

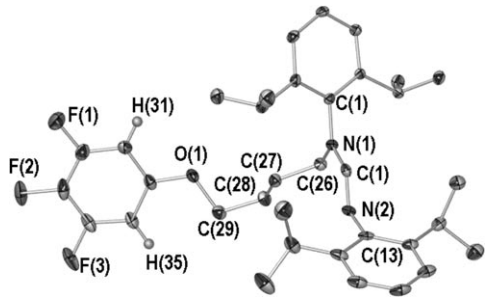

Figure 9. Molecular structure of functionalised DippForm co-product **8**. All hydrogen atoms, excepting H(31) and H(35), omitted. Selected bond lengths (Å) and angles (°): N(1)–C(1) 1.361(4), N(2)–C(1) 1.282(4), N(1)–C(26) 1.464(4), C(29)–O(1) 1.452(4), N(1)-C(1)-N(2) 122.3(3).

with discrete single (N(1)–C(1) 1.361(4) Å) and double (N(2)–C(25) 1.282(4) Å) C–N bonds tethered to a 3,4,5-trifluorophenyl group by a ring opened THF similar to the structure of the 2,3,4,5-tetrafluorophenyl analogue.[10] The ring-opened THF bonds to the aromatic residue through the O atom and the *N,N′*-bis(aryl)formamidine fragment through a C atom. This composition is borne out by C–O and N–C bond lengths about the ring-opened THF tether and is consistent with ^{1}H, ^{13}C and ^{19}F NMR data (see Experimental Section).

Conclusion

N,N′-Bis(aryl)formamidinates provide a range of sterically tunable cyclopentadienyl replacement ligands for Ln^{3+} ions, and the parent *N,N′*-bis(aryl)formamidines can alter the outcome of redox transmetallation/ligand exchange syntheses by variation of their bulkiness. Thus, novel tris(formamidinato)lanthanoid(III) complexes have been isolated by redox transmetallation/ligand exchange reactions of the lanthanoid metals with bis(pentafluorophenyl)mercury and the *N,N′*-bis(aryl)formamidines *o*-TolFormH, XylFormH, MesFormH, EtFormH and *o*-PhPhFormH. The by-product **1YbOH** was isolated during preparation of **1Yb** due to partial hydrolysis. **1YbOH** is the first crystallographically characterised example of a hydroxyl-bridged lanthanoid *N,N′*-bis(aryl)formamidinate complex. We are examining alternatives to mercurials in redox transmetallation (see for example, use of $SnMe_3L$ reagents[37]). Less toxic triarylbismuth compounds have lower or less satisfactory reactivity.[38] X-ray crystallographic studies show exclusively *N,N′*-chelating formamidinate bonding despite the availability of other bonding modes for this family of ligands.[4] A variety of significant differences in coordination number were observed upon progression from the less sterically bulky *o*-TolForm to the more sterically hindered EtForm and *o*-PhPhForm ligands. *N,N′*-Bis(aryl)formamidinates bearing 2,6-dimethyl-, 2-phenyl or 2,6-diethylphenyl groups induce homoleptic trigonal prismatic $[Ln(Form)_3]$ complexes. Extension of the series to *N,N′*-bis(2,6-diisopropylphenyl)formamidinate enables steric inhibition of the final protolytic ligand exchange [Eq. (3)]. This generates the heteroleptic terminal fluoride complexes **6Ln** and ring-opened THF co-products consistent with trapping of a polyfluorobenzyne species, their formation arising from C–F activation of a co-ordinated polyfluorophenyl. Consequently, a new route to heteroleptic fluorides for lanthanoids without a readily accessible Ln^{II} state has been established. The successful isolation of the phenylethynylorganometallics **9Nd** and **9Sm** from analogous syntheses support the intermediacy of $[Ln(DippForm)_2(C_6F_5)]$ complexes. It is proposed that the eliminated polyfluorobenzyne inserts into the $Ln–O_{thf}$ bond, resulting in ring-opening of the coordinated THF followed by reaction with unreacted DippFormH and protolysis to give the functionalised formamidines **7** or **8**. Ring opening of THF has not previously been associated with polyfluorophenylorganometallic compounds. The six-coordinate monomeric structures of $[Ln(DippForm)_2X(thf)]$ (X = F or C≡CPh) feature rare (for Ln^{3+}) terminal Ln–X bonds, plausibly arising from the bulkiness of the DippForm ligands.

Experimental Section

o-TolFormH, XylFormH, MesFormH, EtFormH, *o*-PhPhFormH and DippFormH were synthesised according to a published procedure.[7] Lanthanoid metals were purchased from Tianjiao (Baotou, China) or Santoku as metal ingots, stored under purified nitrogen and freshly filed prior to use. Bis(pentafluorophenyl)mercury,[39a] bis(phenylethynyl)mercury,[39b] and $[Sm(DippForm)_2(thf)_2]$[8] were prepared as reported. (*Caution*: diarylmercurials should be handled in a well-ventilated fume cupboard wearing protective gloves and residues should be included in heavy metal waste or recycled as mercury metal.) *n*-Butyllithium (1.6 M in hexane)

was purchased from Aldrich and stored under nitrogen. Tetrahydrofuran (THF) was pre-dried over sodium wire and freshly distilled over sodium benzophenone ketyl under nitrogen. Hexane and toluene were pre-dried over sodium and distilled over sodium under nitrogen. All manipulations were performed by using conventional Schlenk and glovebox techniques under an atmosphere of purified nitrogen. Infrared spectra (4000–500 cm^{-1}) of Nujol mulls were recorded using a Perkin–Elmer 1600 Fourier transform infrared spectrometer. ^1H NMR spectra of solutions in C_6D_6 were generally recorded at 300.13 MHz and $^{13}C\{^1H\}$ NMR spectra were generally recorded at 75.47 MHz by using a Bruker AC 300 spectrometer at 300 K. Where stated otherwise, spectra were recorded on a Bruker AC 400 spectrometer at 300 K. Chemical shifts were referenced to the residual ^1H and ^{13}C resonances of [D_6]benzene. All microanalyses were by the Campbell Microanalytical Laboratory, Chemistry Department, University of Otago, Dunedin, New Zealand. Metal analyses were by EDTA titrations with Xylenol Orange indicator following acid digestion and buffering. Melting points were determined in sealed glass capillaries under nitrogen and are uncalibrated.

[La(*o*-TolForm)$_3$(thf)$_2$]·2.5THF (1La): THF (40 mL) was added to a Schlenk flask charged with excess freshly filed La metal (0.20 g, 1.47 mmol), $Hg(C_6F_5)_2$ (0.55 g, 1.04 mmol) and *o*-TolFormH (0.35 g, 1.60 mmol), under purified nitrogen. The slurry was stirred at ambient temperature for 72 h before the light brown solution was filtered from the deposit of elemental mercury and an excess of La metal. Solvent was removed in vacuo to give a white powder. Recrystallisation from THF (5 mL) and standing at −6 °C for several days gave colourless square crystals (yield: 0.41 g, 89 %). M.p. 160–162 °C; decomp > 300 °C; IR (Nujol): $\tilde{\nu}$ = 3057 (w), 1667 (m), 1596 (m), 1530 (s), 1303 (s), 1222 (m–s), 1187 (m), 1112 (m), 1069 (m), 1031 (m), 1002 (m), 934 (m), 873 (m), 838 (w), 778 (m), 757 (m–s), 720 cm^{-1} (m); ^1H NMR: δ = 1.23 (s, 12H; CH_2, THF), 2.25 (s, 18H; CH_3), 3.49 (s, 12H; OCH_2, THF), 6.69 (d, ^3J(H,H) = 7.3 Hz, 6H; Ar–H), 6.88 (td, ^3J(H,H) = 7.3 Hz, ^3J(H,H) = 1.2 Hz, 6H; Ar–H), 7.03 (m, 12H; Ar–H), 8.64 ppm (s, 3H; NC(H)N); $^{13}C\{^1H\}$ NMR: δ = 17.9 (CH_3), 24.2 (CH_2), 66.9 (OCH_2), 119.6, 121.6, 125.7, 129.0 (Ar–CH), 129.6, 148.9 (Ar–C), 165.0 ppm (NC(H)N); elemental analysis calcd (%) for $C_{53}H_{61}LaN_6O_2$ (loss of THF of solvation, 952.39): C 66.80, H 6.45, N 8.82, La 14.58; elemental analysis calcd (%) for $C_{57}H_{69}LaN_6O_3$ (1 THF of solvation, 1025.12): C 66.79, H 6.78, N 8.20, La 13.55; found: C 64.22, H 6.38, N 8.84, La 15.00.

[Er(*o*-TolForm)$_3$]·THF (1Er): Following the procedure used in **1La**, Er metal (0.30 g, 1.80 mmol), $Hg(C_6F_5)_2$ (0.50 g, 0.93 mmol) and *o*-TolFormH (0.42 g, 1.87 mmol) gave clusters of pink crystals of **1Er** from THF, which were not suitable for X-ray crystallography (yield: 0.21 g, 38 %). M.p. 183–186 °C; decomp > 300 °C; IR (Nujol): $\tilde{\nu}$ = 3055 (w), 1668 (s), 1594 (m), 1287 (s), 1226 (s), 1188 (m), 1112 (m–s), 1047 (w), 1008 (m), 984 (w), 946 (m), 868 (w), 840 (w), 755 (s), 722 (s), 698 cm^{-1} (s); erbium analysis calcd (%) for $C_{49}ErH_{53}N_6O$ (909.26): Er 18.40; found: Er 18.27.

[{Yb(*o*-TolForm)$_2$(μ-OH)(thf)}$_2$]·2THF (1YbOH): A mixture of *o*-TolFormH (0.50 g, 2.23 mmol), $Hg(C_6F_5)_2$ (0.60 g, 1.11 mmol) and an excess of Yb metal (0.20 g, 1.15 mmol) was dissolved in THF (50 mL). The colourless suspension was left stirring to give a deep red solution that was left stirring overnight. During this time liquid mercury deposited. The deep red solution was filtered through a cannula and a black precipitate remained. The red filtrate was evaporated under vacuum and a yellow precipitate was observed. The remaining red solution was filtered through a cannula and left to crystallise at room temperature. Yellow single crystals were isolated from the red solution and identified by X-ray crystallography as [{Yb(*o*-TolForm)$_2$(μ-OH)(thf)}$_2$]·2THF (yield: 0.31 g, 20 %). M.p. 200 °C; IR (Nujol): $\tilde{\nu}$ = 3666 (m; O–H str), 1667 (m), 1594 (m), 1532 (s), 1223 (m–s), 1190 (m), 1111 (m), 1067 (m), 1020 (m), 991 (w), 945 (m), 870 (m), 840 (w), 795 (w), 776 (m), 757 (m), 720 (m), 694 cm^{-1} (m); elemental analysis calcd (%) for $C_{68}H_{78}N_8O_4Yb_2$ (loss of THF of solvation, 1417.51): C 57.62, H 5.51, N 7.90, Yb 24.27; found: C 57.86, H 5.47, N 7.75, Yb 24.03.

[Yb(*o*-TolForm)$_3$(thf)] (1Yb): *n*-Butyllithium (1.18 mL, 1.88 mmol) was added dropwise to a solution of *o*-TolFormH (0.46 g, 1.88 mmol) in THF (30 mL), resulting in the formation of a light green solution that was stirred at ambient temperature for 2 h. The light green solution was added to a $YbCl_3$ (0.18 g, 0.63 mmol) slurry in THF (30 mL), giving a yellow suspension that was left to stir overnight at ambient temperature. The yellow suspension was filtered, volatiles were removed in vacuo and the yellow material was extracted into hexane (15 mL) and concentrated in vacuo (3 mL) to give yellow rectangular single crystals (yield: 0.41 g, 72 %). M.p. 142–144 °C; decomp > 300 °C; IR (Nujol): $\tilde{\nu}$ = 2724 (w), 1667 (m), 1537 (s), 1294 (s), 1231 (s), 1189 (m), 1111 (m–s), 1047 (w), 1017 (m), 987 (m), 946 (m), 866 (w), 842 (w), 797 (w), 753 (s), 718 cm^{-1} (s); ^1H NMR: δ = −7.01 (br s, 3H; NC(H)N), 1.97 (br s, 4H; CH_2, THF), 4.45 (br s, 4H; OCH_2, THF), 5.52 (s, 18H; CH_3), 8.00 (br s, 12H; Ar–H), 10.08 (br s, 6H; Ar–H), 12.26 ppm (br s, 6H; Ar–H); elemental analysis calcd (%) for $C_{49}H_{53}N_6OYb$ (915.01): C 64.32, H 5.84, N 9.18, Yb 18.91; found: C 63.95, H 5.74, N 9.12, Yb 18.40.

[La(XylForm)$_3$(thf)]·2THF (2La): Following a similar procedure to that for **1La**, La metal (0.20 g, 1.47 mmol), $Hg(C_6F_5)_2$ (0.50 g, 0.93 mmol) and XylFormH (0.47 g, 1.86 mmol) gave colourless rectangular crystals from THF (yield: 0.43 g, 86 %). M.p. 218–220 °C; decomp 284 °C; IR (Nujol): $\tilde{\nu}$ = 1651 (m–s), 1594 (m–s), 1538 (s), 1290 (s), 1230 (m), 1198 (s), 1093 (m), 1069 (m), 1021 (m), 982 (w), 934 (m), 864 (w), 822 (w), 762 (s), 699 cm^{-1} (m); ^1H NMR (400.13 MHz, C_6D_6, 300 K): δ = 1.40 (s, 12H; CH_2), 2.04 (s, 36H; CH_3), 3.55 (s, 12H; OCH_2), 6.83–6.90 (m, 18H; Ar–H), 8.01 ppm (s, 3H; NC(H)N); $^{13}C\{^1H\}$ NMR (100.62 MHz, C_6D_6, 300 K): δ = 19.1 (CH_3), 26.1 (CH_2, THF), 68.2 (OCH_2, THF), 124.0, 129.0 (Ar–CH), 131.9, 149.1 (Ar–C), 169.8 ppm (NC(H)N); elemental analysis calcd (%) for $C_{63}H_{81}LaN_6O_3$ (1109.25): C 68.22, H 7.36, N 7.58, La 12.52; found: C 67.06, H 7.31, N 7.66, La 13.07.

[Sm(XylForm)$_3$] (2Sm): Following a similar procedure to that for **1La**, Sm metal (0.20 g, 1.28 mmol), $Hg(C_6F_5)_2$ (0.50 g, 0.93 mmol) and XylFormH (0.35 g, 1.38 mmol) gave yellow rectangular crystals from THF (yield: 0.33 g, 80 %). M.p. 294–298 °C; decomp > 360 °C; IR (Nujol): $\tilde{\nu}$ = 1651 (m–s), 1594 (m–s), 1519 (s), 1263 (s), 1230 (s), 1202 (s), 1092 (m), 1006 (w), 980 (w), 942 (s), 918 (w), 822 (w), 762 (s), 698 cm^{-1} (s); ^1H NMR (400.13 MHz, C_6D_6, 300 K): δ = 1.43 (s, 36H; CH_3), 6.43 (d, ^3J(H,H) = 7.5 Hz, 12H; *m*-Ar–H), 6.76 (t, ^3J(H,H) = 7.5 Hz, 6H; *p*-Ar–H), 10.92 ppm (s, 3H; NC(H)N); $^{13}C\{^1H\}$ NMR (100.62 MHz, C_6D_6, 300 K): δ = 20.1 (CH_3), 123.5, 129.0 (Ar–CH), 131.1, 147.0 (Ar–C), 190.8 ppm (NC(H)N); elemental analysis calcd (%) for $C_{51}H_{57}N_6Sm$ (904.38): C 67.73, H 6.35, N 9.29, Sm 16.63; found: C 66.61, H 6.59, N 9.18, Sm 16.07.

[La(MesForm)$_3$]·2THF (3La): Following the procedure used for **1La**, La metal (0.20 g, 1.47 mmol), $Hg(C_6F_5)_2$ (0.31 g, 0.59 mmol) and MesFormH (0.25 g, 0.89 mmol) gave colourless square crystals from THF (yield: 0.29 g, 87 %). M.p. 256–260 °C; decomp > 360 °C; IR (Nujol):$\tilde{\nu}$ = 2732 (w), 1652 (m), 1602 (s), 1266 (w), 1230 (s), 1166 (w), 1074 (w), 1029 (w), 1006 (w), 950 (m–s), 923 (m–s), 850 (w), 830 (m), 794 (w), 756 (s), 698 (s), 616 (w), 560 (w), 517 cm^{-1} (w); ^1H NMR (400.13 MHz, C_6D_6, 300 K): δ = 1.39 (t, ^3J(H,H) = 6.3 Hz, 8H; CH_2, THF), 2.09 (s, 36H; *o*-CH_3), 2.15 (s, 18H; *p*-CH_3), 3.56 (t, ^3J(H,H) = 6.1 Hz, 8H; OCH_2, THF), 6.71 (s, 12H; Ar–H), 8.15 ppm (s, 3H; NC(H)N); $^{13}C\{^1H\}$ NMR (100.62 MHz, C_6D_6, 300 K) δ = 19.9, 21.1 (CH_3), 26.1 (CH_2), 68.2 (OCH_2), 129.5 (Ar–CH), 131.7, 132.6, 146.8 (Ar–C), 170.1 ppm (NC(H)N); lanthanum analysis calcd (%) for $C_{65}H_{85}LaN_6O_2$ (1121.33): La 12.39; found: La 12.17.

[Nd(MesForm)$_3$]·2toluene (3Nd): Following the procedure used for **1La**, Nd metal (0.30 g, 2.08 mmol), $Hg(C_6F_5)_2$ (0.50 g, 0.94 mmol) and MesFormH (0.40 g, 1.42 mmol) gave blue rectangular crystals following crystallisation of the crude product from toluene (3 mL) (yield: 0.30 g, 65 %). M.p. 318–320 °C; decomp > 360 °C; IR (Nujol):$\tilde{\nu}$ = 2729 (w), 1645 (m), 1604 (s), 1529 (m), 1305 (m), 1279 (m), 1230 (s), 1156 (w), 1030 (w), 1009 (w), 951 (m), 914 (m), 851 (m), 756 (s), 729 (s), 698 cm^{-1} (s); ^1H NMR (400.13 MHz, C_6D_6, 300 K): δ = 0.61 (br s, 36H; *o*-CH_3), 2.45 (s, 18H; *p*-CH_3), 6.60 (s, 12H; Ar–H), 9.03 ppm (s, 3H; NC(H)N); $^{13}C\{^1H\}$ NMR δ = 13.2, 21.2 (CH_3), 126.4 (Ar–CH), 129.6, 136.3, 140.6, (Ar–C), 169.9 ppm (NC(H)N); elemental analysis calcd (%) for $C_{57}H_{69}N_6Nd$ (loss of toluene of solvation, 982.46): C 69.69, H 7.08, N 8.55, Nd 14.68; found: C 69.22, H 7.08, N 8.43, Nd 14.45.

[Sm(MesForm)$_3$] (3Sm): Following a similar procedure to that used for compound **1La**, Sm metal (0.25 g, 1.60 mmol), $Hg(C_6F_5)_2$ (0.22 g, 0.41 mmol) and MesFormH (0.23 g, 0.82 mmol) gave yellow square block crystals of **3Sm** from hexane (yield: 0.29 g, 71 %). M.p. 200–204 °C; IR

(Nujol): $\tilde{\nu}$ = 2727 (w–m), 1646 (m), 1609 (m), 1532 (s), 1306 (s), 1277 (s), 1213 (s), 1156 (s), 1030 (m), 1007 (m), 964 (m), 913 (s), 879 (w), 851 (s), 795 (w), 756 (s), 699 (s), 606 (w), 468 cm^{-1} (w); ^1H NMR (400.13 MHz, C_6D_6, 300 K): δ = 1.54 (s, 36H; *o*-CH_3), 1.96 (s, 18H; *p*-CH_3), 6.49 (s, 12H; Ar–H), 11.11 ppm (s, 3H; NC(H)N); $^{13}C\{^1H\}$ NMR: δ = 20.2, 21.3 (CH_3), 129.6 (Ar–CH), 130.9, 132.1, 144.6 (Ar–C), 191.8 ppm (NC(H)N); samarium analysis calcd (%) for $C_{57}H_{69}N_6Sm$ (988.58): Sm 15.21; found: Sm 15.36.

[Yb(MesForm)$_3$] (3Yb): Following the procedure used for **1La**, Yb metal (0.20 g, 1.13 mmol), $Hg(C_6F_5)_2$ (0.28 g, 0.52 mmol) and MesFormH (0.22 g, 0.79 mmol) gave orange rectangular crystals from THF (5 mL) (yield: 0.21 g, 81%). M.p. 280–284°C; decomp > 300°C; IR (Nujol): $\tilde{\nu}$ = 2728 (w), 1640 (m), 1605 (m), 1532 (s), 1306 (w), 1274 (m), 1229 (s), 1160 (w), 1030 (w), 1010 (w), 964 (w), 952 (m), 922 (w), 851 (m–s), 830 (w), 795 (w), 756 (m–s), 698 cm^{-1} (s); ^1H NMR: δ = −6.26 (brs, 3H; NC(H)N), 0.29 (s, 18H; *p*-CH_3), 3.32 (s, 36H; *o*-CH_3), 8.35 ppm (s, 12H; Ar–H); $^{13}C\{^1H\}$ NMR (100.62 MHz, C_6D_6, 300 K): δ = 19.6, 21.9 (CH_3), 129.8 (Ar–CH), 133.0, 135.6, 141.9 (Ar–C), 169.1 ppm (NC(H)N); elemental analysis calcd (%) for $C_{57}H_{69}N_6Yb$ (1011.22): C 67.70, H 6.88, N 8.31, Yb 17.11; found: C 67.13, H 6.61, N 8.16, Yb 17.34.

[La(EtForm)$_3$]·2THF (4La): Following the procedure used for **1La**, La metal (0.25 g, 1.83 mmol), $Hg(C_6F_5)_2$ (0.35 g, 0.62 mmol) and EtFormH (0.30 g, 0.97 mmol) gave colourless rectangular crystals from THF (3 mL) (yield: 0.28 g, 82%). M.p. 228–232°C; IR (Nujol): $\tilde{\nu}$ = 2732 (sh w), 1667 (m), 1601 (m), 1292 (w), 1260 (w), 1230 (s), 1105 (w), 1073 (w), 1030 (w), 1008 (w), 942 (m), 923 (m), 830 (m), 795 (m), 756 (s), 698 (s), 616 (w), 559 (w), 517 cm^{-1} (w); ^1H NMR: δ = 1.07 (t, ^3J(H,H) = 7.5 Hz, 36H; CH_3), 2.69 (q, ^3J(H,H) = 7.5 Hz, 24H; CH_2), 7.15–7.17 (brm, 18H; Ar–H), 8.39 ppm (s, 3H; NC(H)N); $^{13}C\{^1H\}$ NMR: δ = 13.6 (CH_3), 24.3 (CH_2), 123.1, 124.7 (Ar–CH), 136.3, 146.7 (Ar–C), 169.2 ppm (NC(H)N); elemental analysis calcd (%) for $C_{63}H_{81}LaN_6$ (loss of THF of solvation, 1061.28): C 71.30, H 7.69 N, 7.92, La 13.09; elemental analysis calcd (%) for $C_{67}H_{89}N_6OLa$ (1THF of solvation, 1133.39): C 71.00, H 7.91, N 7.41, La 12.26; found: C 69.60, H 7.61, N 7.42, La 12.70.

[Nd(EtForm)$_3$]·2THF (4Nd): Following the procedure used for **1La**, Nd metal (0.20 g, 1.38 mmol), $Hg(C_6F_5)_2$ (0.35 g, 0.67 mmol) and EtFormH (0.31 g, 1.00 mmol) gave blue rectangular crystals from THF (5 mL) (yield: 0.27 g, 77%). M.p. 156–160°C; decomp > 250°C; IR (Nujol): $\tilde{\nu}$ = 2731 (sh w), 1665 (m–s), 1594 (m–s), 1520 (s), 1287 (s), 1231 (m), 1196 (s), 1105 m 1071 (m–s), 1032 (w), 1010 (w), 942 (s), 922 (w), 869 (w), 827 (w), 797 (m), 756 (s), 698 cm^{-1} (s); ^1H NMR: δ = 0.48 (brs, 24H; CH_2), 0.79 (brs, 36H; CH_3), 5.91 (t, ^3J(H,H) = 7.0 Hz, 6H; *p*-Ar–H), 6.90 (d, ^3J(H,H) = 7.0 Hz, 12H; *m*-Ar–H), 8.21 ppm (s, 3H; NC(H)N); $^{13}C\{^1H\}$ NMR: δ = 16.1 (CH_3), 19.3 (CH_2), 123.4, 127.8 (Ar–CH), 136.8, 146.4 (Ar–C), 172.2 ppm (NC(H)N); elemental analysis calcd (%) for $C_{63}H_{81}N_6Nd$ (loss of THF of solvation, 1066.62): C 70.94, H 7.65 N, 7.88, Nd 13.52; found: C 69.67, H 7.79, N 7.66, Nd 13.69.

[Sm(EtForm)$_3$]·2THF (4Sm): Following the procedure used for **1La**, Sm metal (0.30 g, 1.92 mmol), $Hg(C_6F_5)_2$ (0.29 g, 0.54 mmol) and EtFormH (0.38 g, 0.72 mmol) gave yellow rectangular crystals from THF (5 mL) (yield: 0.22 g, 88%). M.p. 258–260°C; decomp > 360°C; IR (Nujol): $\tilde{\nu}$ = 2727 sh (w), 1667 (m), 1592 (m), 1526 (s), 1288 (s), 1192 (w), 1160 (w), 1197 (s), 1105 (w), 1073 (m), 1034 (w), 1013 (w), 968 (w), 942 (m), 913 (w), 869 (w), 807 (w), 769 (m), 757 (s), 722 (w–m), 668 cm^{-1} (w); ^1H NMR: δ = 0.88 (t, ^3J(H,H) = 7.4 Hz, 36H; CH_3), 1.75 (q, ^3J(H,H) = 6.6 Hz, 24H; CH_2), 6.76 (d, ^3J(H,H) = 7.6 Hz, 12H; *m*-Ar–H), 6.95 (t, ^3J(H,H) = 7.6 Hz, 6H; *p*-Ar–H), 11.31 ppm (s, 3H; NC(H)N); $^{13}C\{^1H\}$ NMR: δ = 15.0 (CH_3), 26.1 (CH_2), 124.2, 126.4 (Ar–CH), 137.0, 145.9 (Ar–C), 192.4 ppm (NC(H)N); elemental analysis calcd (%) for $C_{63}H_{81}N_6Sm$ (loss of THF of solvation, 1072.74): C 70.54, H 7.61 N, 7.83, Sm 14.02; found: C 69.87, H 8.01, N 7.43, Sm 13.96.

[Ho(EtForm)$_3$]·2THF (4Ho): Following the procedure used for **1La**, Ho metal (0.20 g, 1.21 mmol), $Hg(C_6F_5)_2$ (0.37 g, 0.69 mmol) and EtFormH (0.32 g, 1.04 mmol) gave pink crystals from THF (2 mL) (yield: 0.12 g, 33%). M.p. 160–162°C; IR (Nujol): $\tilde{\nu}$ = 1646 (s), 1587 (m), 1527 (s), 1284 (s), 1199 (s), 1105 (m), 1033 (w), 966 (w), 944 (m), 935 (w), 868 w-m, 807 (m), 770 (m–s), 757 (m–s), 721 (w), 471 cm^{-1} (w); holmium analysis calcd (%) for $C_{63}H_{81}N_6Ho$ (loss of THF of solvation, 1087.31): Ho 15.32; found: Ho 15.17.

[Yb(EtForm)$_3$]·2THF (4Yb): Following the procedure used for **1La**, Yb metal (0.30 g, 1.73 mmol), $Hg(C_6F_5)_2$ (0.47 g, 0.89 mmol) and EtFormH (0.41 g, 1.34 mmol) gave orange rectangular crystals from THF (4 mL) (yield: 0.21 g, 38%). M.p. > 360°C; IR (Nujol): $\tilde{\nu}$ = 2732 (sh w), 1666 (s), 1589 (s), 1537 (s), 1283 (s), 1260 sh (w), 1188 (m), 1104 (m), 1071 (m), 1032 (w), 946 (w), 869 (w), 804 (m), 757 (s), 721 (w–m), 466 cm^{-1} (w); ^1H NMR (400.13 MHz, C_6D_6, 300 K): δ = −3.75 (brs, 3H; NC(H)N), 0.74 (brs, 60H; CH_2 and CH_3), 1.39 (brs, 8H; CH_2, THF), 3.57 (brs, 8H; OCH_2, THF), 7.80 (t, ^3J(H,H) = 7.0 Hz, 6H; *p*-Ar–H), 8.73 ppm (brs, 12H; *m*-Ar–H); $^{13}C\{^1H\}$ NMR (100.61 MHz, C_6D_6, 300 K): δ = 16.0 (CH_3), 25.4 (CH_2, THF), 36.7 (CH_2), 68.5 (OCH_2, THF), 127.1, 127.4 (Ar–CH), 136.9, 147.6 (Ar–C), 167.9 ppm (NC(H)N); elemental analysis calcd (%) for $C_{71}H_{97}N_6O_2Yb$ (retention of two THF of solvation, 1239.59): C 68.79, H 7.78, N 6.78, Yb 13.96; found: C 67.97, H 7.49, N 6.71, Yb 13.62.

[La(*o*-PhPhForm)$_3$] (5La): Following a similar procedure to that used for compound **1La**, La metal (0.30 g, 2.20 mmol), $Hg(C_6F_5)_2$ (0.57 g, 1.07 mmol) and *o*-PhPhFormH (0.56 g, 1.61 mmol) were used in the reaction. The crude product was crystallised from toluene giving, after drying in vacuo, a white powder (yield: 0.40 g, 70%). M.p. 262–266°C; IR (Nujol): $\tilde{\nu}$ = 2732 (w), 1664 (s), 1590 (s), 1521 (s), 1303 (s), 1262 (w), 1229 (s), 1111 (w), 945 (m), 757 (s), 744 (m), 728 (w), 698 cm^{-1} (s); elemental analysis calcd (%) for $C_{75}H_{57}LaN_6$ (1181.22): C 76.26, H 4.86, N 7.11, La 11.76; found: C 75.97, H 4.69, N 7.13, La 11.66. All **5Ln** compounds were insufficiently soluble for an adequately resolved NMR spectrum.

[Nd(*o*-PhPhForm)$_3$] (5Nd): Following the procedure for **1La**, Nd metal (0.40 g, 2.77 mmol), $Hg(C_6F_5)_2$ (0.39 g, 0.73 mmol) and *o*-PhPhFormH (0.38 g, 1.10 mmol) gave a blue powder (yield: 0.32 g, 73%). M.p. 248–252°C; IR (Nujol): $\tilde{\nu}$ = 2733 (w), 1662 (s), 1588 (m), 1522 (m), 1305 (s), 1261 (w), 1203 (m), 1111 (w), 944 (m), 761 (m), 744 (m), 726 (m), 694 cm^{-1} (m); elemental analysis calcd (%) for $C_{75}H_{57}N_6Nd$ (1186.56): C 75.92, H 4.84, N 7.08, Nd 12.16; found: C 75.68, H 4.89, N 7.12, Nd 11.96.

[Sm(*o*-PhPhForm)$_3$]·toluene (5Sm): Following the procedure for **1La**, Sm metal (0.30 g, 1.92 mmol), $Hg(C_6F_5)_2$ (0.39 g, 0.74 mmol) and *o*-PhPhFormH (0.39 g, 1.12 mmol) gave yellow rectangular crystals after crystallisation of the crude product from toluene (4 mL) (yield: 0.32 g, 82%). M.p. 248–252°C; IR (Nujol): $\tilde{\nu}$ = 2733 (w), 1664 (s), 1599 (s), 1519 (s), 1300 (s), 1262 (w), 1229 (s), 1113 (w), 1072 (w), 1050 (w), 1006 (w), 946 (m), 923 (w), 829 (w), 794 (w), 757 (s), 744 (m), 728 (w), 698 cm^{-1} (s); elemental analysis calcd (%) for $C_{82}H_{65}N_6Sm$ (lattice toluene retained, 1284.75): C 76.66, H 5.10, N 6.54, Sm 11.70; found: C 75.81, H 5.10, N 6.59, Sm 11.45.

[Er(*o*-PhPhForm)$_3$] (5Er): Following the procedure for **1La**, Er metal (0.40 g, 2.77 mmol), $Hg(C_6F_5)_2$ (0.39 g, 0.73 mmol) and *o*-PhPhFormH (0.38 g, 1.10 mmol) gave **5Er** as a pink powder (yield: 0.48 g, 86%). M.p. 260–264°C; IR (Nujol): $\tilde{\nu}$ = 3020 (w), 1664 (s), 1590 (m), 1564 (m), 1301 (s), 1262 (m), 1208 (s), 1178 (w), 1154 (w), 1115 (w), 1072 (w), 1053 (w), 1008 (w), 950 (m), 913 (w), 829 (w), 760 (s), 744 (m), 728 (w), 698 cm^{-1} (s); erbium analysis calcd (%) for $C_{75}H_{57}N_6Er$ (1209.58): Er 13.83; found: Er 13.77.

[La(DippForm)$_2$F(thf)]·toluene (6La)

Method 1: THF (20 mL) was added to a Schlenk flask charged with freshly filed La metal (0.14 g, 1.01 mmol), $Hg(C_6F_5)_2$ (0.37 g, 0.69 mmol) and DippFormH (0.33 g, 0.91 mmol) under a purified nitrogen atmosphere. The colourless slurry was stirred at ambient temperature for 24 h resulting in a noticeable colour change to light yellow. Filtration, to remove deposited elemental mercury and excess La metal, followed by removal of volatiles in vacuo gave a pale yellow solid that was purified by recrystallisation from toluene (10 mL) at −30°C (yield: 0.26 g, 55%). M.p. 283–285°C (decomp) (lit. 284°C, also decomp).[10] IR absorption consistent with original preparation.[10] IR (Nujol): $\tilde{\nu}$ = 2713 (w), 1925 (w), 1858 (w), 1798 (w), 1662 (s), 1608 (s), 1586 (s), 1317 (m), 1270 (m), 1185 (s), 1104 (s), 1049 (m), 1019 (m), 801 (m), 759 (s), 730 (s), 697 (s), 672 cm^{-1} (w); elemental analysis (vacuum dried sample) calcd (%) for $C_{54}H_{78}FLaN_4O$ (no toluene of crystallisation, 962.46): La 14.51; found: La 14.58.

Method 2: Following the procedure for Method 1, freshly filed La metal (0.10 g, 0.72 mmol), Hg(*o*-HC_6F_4)$_2$ (0.34 g, 0.68 mmol) and DippFormH (0.50 g, 1.37 mmol) gave colourless elongated hexagonal plates in three batches (combined yield: 0.40 g, 84%). M.p. 284°C (decomp) (lit. 284°C, also decomp).[10] ^{1}H and ^{19}F NMR and IR absorption data consistent with previously reported data.[10]

***N,N′*-Bis(2,6-diisopropylphenyl)-*N*-{4-(3′,4′,5′-trifluorophenoxy)butyl}formamidine (8)**: Compound obtained as co-product from [Ln(DippForm)$_2$F(thf)] syntheses undertaken by using three equivalents of DippFormH and the mercurial Hg(*o*-HC_6F_4)$_2$ (Ln = La, Nd and Sm). Representative isolation: The vacuum dried filtrate following isolation of [La(DippForm)$_2$F(thf)]·toluene from Method 2 was hydrolysed with reagent grade diethyl ether (50 mL) and water (50 mL), gravity filtered and separated. Drying of the organic phase over anhydrous $MgSO_4$ followed by solvent evaporation under reduced pressure (ca. 10 mL) afforded DippForm$(CH_2)_4$O(3,4,5-$F_3C_6H_2$) (**8**) as colourless rods (0.19 g, 74%). M.p. 156°C; IR (Nujol): $\tilde{\nu}$ = 1665 (s), 1633 (s), 1528 (m), 1289 (m), 1230 (s), 1150 (w), 1098 (m), 950 (m), 923 (m), 821 (w), 756 (s), 728 (s), 689 (s), 676 cm^{-1} (w); ^{1}H NMR: δ = 1.18 (d, ^3J(H,H) = 6.9 Hz, 6H; CH_3, *i*Pr), 1.31 (d, ^3J(H,H) = 6.9 Hz, 6H; CH_3, *i*Pr), 1.40 (d, ^3J(H,H) = 6.9 Hz, 12H; CH_3, *i*Pr), 1.53 (m, 2H; CH_2), 1.96 (m, 2H; CH_2), 3.33 (m, 2H; NCH_2), 3.39 (sept, ^3J(H,H) = 6.9 Hz, 2H; CH, *i*Pr), 3.57 (sept, ^3J(H,H) = 6.9 Hz, 2H; CH, *i*Pr), 3.89 (m, 2H; OCH_2), 6.17 (dd, ^3J(H,F) = 9.9 Hz, ^4J(H,F) = 6.1 Hz, 2H; Ar_F-2,6-H_2), 7.03–7.30 ppm (m, 7H; Ar–H and NC(H)N); ^{13}C{^{1}H} NMR: δ = 24.5, 24.9 (CH_3, *i*Pr), 25.4 (CH_2), 25.7 (CH_3, *i*Pr), 27.3 (CH_2), 28.8, 29.0 (CH, *i*Pr), 50.6 (NCH_2), 69.6 (OCH_2), 99.6 (Ar_F-2,6-C, ^2J(C,F) = 23.0 Hz), 123.5, 123.7, 124.9, 125.0 (Ar–CH), 140.0, 143.4, 146.9, 148.6 (Ar–C), 151.9 ppm (NCN) (carbon resonances for the fluoroarene group, excepting the 2,6-CH resonance, not observed); ^{19}F NMR (282.38 MHz, C_6D_6, 303 K, CCl_3F); δ = −170.8 (tt, ^3J(F,F) = 21.2 Hz, ^4J(F,H) = 6.1 Hz, 1F; Ar_F-F4′), −133.3 ppm (dd, ^3J(F,F) = 21.2 Hz, ^3J(F,H) = 9.9 Hz, 2F; Ar_F-F3,5′); elemental analysis calcd (%) for $C_{35}H_{45}F_3N_2O$ (566.73): C 74.17, H 8.00, N 4.94; found: C 73.91, H 7.74, N 5.04.

[Ce(DippForm)$_2$F(thf)]·toluene (6Ce): Following a similar procedure to that for [La(DippForm)$_2$F(thf)]·toluene method 1, Ce metal (0.20 g, 1.43 mmol), Hg(C_6F_5)$_2$ (0.37 g, 0.69 mmol) and DippFormH (0.51 g, 1.40 mmol) gave colourless irregular prisms of **6Ce** on recrystallisation from toluene (5 mL) at −5°C (yield: 0.19 g, 39%). M.p. 273°C (decomp); IR (Nujol): $\tilde{\nu}$ = 1937 (w), 1862 (w), 1797 (w), 1668 (s), 1638 (s), 1600 (m), 1587 (m), 1525 (s), 1287 (s), 1231 (s), 1188 (s), 1098 (m), 1054 (m), 1010 (m), 935 (s), 872 (w), 822 (m), 800 (m), 756 (s), 728 (m), 697 (m), 673 cm^{-1} (w); cerium analysis calcd (%) for $C_{61}CeH_{86}FN_4O$ (1050.46) (value in parentheses for $C_{54}H_{78}CeFN_4O$ with no toluene of crystallisation, 958.34): Ce 13.34 (14.62); found: Ce 13.47.

[Nd(DippForm)$_2$F(thf)]·toluene (6Nd·tol) and [Nd(DippForm)$_2$F(thf)] (6Nd)

Method 1: THF (20 mL) was added to a Schlenk flask charged with freshly filed Nd metal (0.12 g, 0.83 mmol), Hg(C_6F_5)$_2$ (0.37 g, 0.69 mmol) and DippFormH (0.51 g, 1.40 mmol) under a purified nitrogen atmosphere. The resulting slurry was stirred at ambient temperature for 24 h to yield a blue-aquamarine solution with a metallic deposit. Filtration followed by removal of volatiles in vacuo gave an aquamarine solid that was recrystallised from toluene (10 mL) at −30°C to give both rhombohedral (no toluene) and irregular (toluene of crystallisation) blue-green prisms in several batches (combined yield: 0.33 g, 68% based on [Nd(DippForm)$_2$F(thf)]·toluene). M.p. 276–278°C (decomp); IR (Nujol): $\tilde{\nu}$ = 1941 (w), 1871 (w), 1798 (w), 1662 (s), 1639 (s), 1588 (m), 1522 (s), 1279 (s), 1233 (s), 1178 (m), 1153 (m), 1098 (m), 1046 (s), 1009 (m), 933 (m), 873 (w), 822 (w), 800 (m), 757 (m), 728 (w), 698 (m), 669 cm^{-1} (w); ^{1}H NMR: δ = −9.97 (brs, 2H; NC(H)N), −4.96 (brs, 8H; CH, *i*Pr), 1.37 (brs, 4H; CH_2, THF), 2.13 (s, 3H; CH_3, toluene), 2.28 (brs, 48H; CH_3, *i*Pr), 3.36 (brs, 4H; OCH_2, THF), 6.63 (brs, 4H; *p*-Ar -H), 7.12 (brs, 8H; *m*-Ar–H), 7.17–7.26 (m, 5H; Ar–H, toluene); elemental analysis calcd (%) for $C_{61}H_{86}FN_4NdO$ (1054.58) (values in parentheses for $C_{54}H_{78}FN_4NdO$ with no toluene of crystallisation, 962.44): C 69.47 (67.39), H 8.22 (8.17), N 5.31 (5.82), Nd 13.68 (14.99); found: C 67.87, H 8.25, N 5.72, Nd 14.67.

Method 2: Following the procedure for Method 1, freshly filed Nd metal (0.16 g, 1.11 mmol), Hg(C_6F_5)$_2$ (0.37 g, 0.69 mmol) and DippFormH (0.33 g, 0.91 mmol) gave both rhombohedral (no toluene) and irregular (toluene of crystallisation) blue-green prisms (yield: 0.34 g, 69% based on [Nd(DippForm)$_2$F(thf)]·toluene). M.p. 276°C (decomp). Unit cell data for the two types of crystalline material consistent with data for structures reported herein.

Method 3: Following the procedure for Method 1, freshly filed Nd metal (0.16 g, 1.11 mmol), Hg(*o*-HC_6F_4)$_2$ (0.34 g, 0.68 mmol) and DippFormH (0.50 g, 1.37 mmol) gave both rhombohedral (no toluene) and irregular (toluene of crystallisation) blue-green prisms (yield: 0.26 g, 54%), m.p. 275–278°C (decomp). Unit cell data for two types of crystalline material consistent with data reported herein.

[Sm(DippForm)$_2$F(thf)] (6Sm)

Method 1: THF (20 mL) was added to a Schlenk flask charged with freshly filed Sm metal (0.06 g, 0.40 mmol), Hg(C_6F_5)$_2$ (0.37 g, 0.69 mmol) and DippFormH (0.33 g, 0.91 mmol) under a purified nitrogen atmosphere. The resulting slurry was stirred at ambient temperature for 36 h to yield a pale yellow solution after filtration. Removal of volatiles gave a light yellow powder that was extracted into toluene (10 mL) and cooled to −30°C to give **6Sm** as light yellow rhombohedral prisms (yield: 0.27 g, 62%). M.p. 276–278°C (decomp); (lit. 276°C, also decomp);[8] ^{1}H and ^{19}F NMR data consistent with those previously reported.[8]

Method 2: Following the procedure for Method 1, freshly filed Sm metal (0.07 g, 0.47 mmol), Hg(*o*-HC_6F_4)$_2$ (0.34 g, 0.68 mmol) and DippFormH (0.50 g, 1.37 mmol) gave light yellow rhombohedral prisms (yield: 0.18 g, 41%). M.p. 275°C (decomp) (lit. 276°C, also decomp);[8] unit cell data consistent with those of the reported structure[8] (a = 20.465, b = 12.203, c = 21.645 Å, β = 110.07°, V = 5077.2 Å^3); samarium analysis calcd (%) for $C_{54}H_{78}FN_4OSm$ (968.58): Sm 15.52; found: Sm 15.01.

[Tm(DippForm)$_2$F(thf)] (6Tm): Following a similar procedure to that for **6La** method 1, Tm metal (0.18 g, 1.07 mmol), Hg(C_6F_5)$_2$ (0.37 g, 0.69 mmol) and DippFormH (0.51 g, 1.40 mmol) gave colourless rhombohedral prisms of **6Tm** upon recrystallisation from toluene (ca. 4 mL) at 0°C (yield: 0.15 g, 33%). M.p. 279°C (decomp); IR (Nujol): $\tilde{\nu}$ = 1936 (w), 1861 (w), 1797 (w), 1661 (s), 1636 (s), 1588 (s), 1261 (m), 1233 (s), 1110 (m), 1097 (s), 1039 (m), 950 (s), 799 (m), 756 (s), 729 (m), 699 (s), 672 cm^{-1} (w); thulium analysis calcd (%) for $C_{54}H_{78}FN_4OTm$ (987.13): Tm 17.11; found: Tm 16.98.

After syntheses of **6Ce**, **6Nd** (method 1), and **6Tm**, the ^{19}F NMR spectra of the reaction mixtures showed the presence of *o*-$HC_6F_4O(CH_2)_4$-(DippForm) (**7**)[10] and C_6F_5H in a 1:2 mole ratio [see Eq. (8)].

[Nd(DippForm)$_2$(CCPh)(thf)]·toluene (9Nd): THF (50 mL) was added to a Schlenk flask charged with neodymium metal filings (0.16 g, 1.11 mmol), bis(phenylethynyl)mercury (0.28 g, 0.70 mmol) and DippFormH (0.50 g, 1.37 mmol) under purified nitrogen. The resulting slurry was stirred at ambient temperature for 24 h to yield a blue-pink solution after filtration to remove elemental mercury and excess metal. Volatiles were removed under reduced pressure to yield an aqua-blue powder. Recrystallisation from toluene (saturated 10 mL solution) gave **9Nd** as blue-pink blocks after standing overnight (yield: 0.29 g, 37%). M.p. 161°C, solvent loss at 102°C; IR (Nujol): $\tilde{\nu}$ = 2059 (m), 1933 (w), 1862 (w), 1795 (w), 1667 (m), 1592 (m), 1520 (s), 1459 (s), 1380 (m), 1360 (m), 1315 (m), 1279 (s), 1239 (m), 1191 (sh m), 1109 (m), 1053 (m), 1024 (m), 941 (m), 869 (m), 801 (m), 770 (m), 756 (m), 730 (w), 692 cm^{-1} (w); ^{1}H NMR: δ = −2.80 (brs, 8H; CH, *i*Pr), −1.88 (brs, 24H; CH_3, *i*Pr), 1.42 (m, 4H; CH_2), 2.18 (s, 3H; CH_3, toluene), 2.32 (brs, 24H; CH_3, *i*Pr), 3.49 (m, 4H; OCH_2), 4.16 (m, 2H; Ar–H, C_6H_5), 5.76 (m, 2H; Ar–H, C_6H_5), 6.11 (m, 1H; Ar–H, C_6H_5), 7.10–7.31 (m, 9H; Ar–H, toluene and *p*-Ar–H), 8.40 (brs, 8H; *m*-Ar–H), 20.48 ppm (brs, 2H; NC(H)N); ^{13}C{^{1}H} NMR: δ = 21.8 (s; CH_3, *i*Pr), 23.2 (s; CH_3, *i*Pr), 24.1 (s; CH_2), 28.7 (s; OCH_2), 29.6 (s; CH, *i*Pr), 118.7 (s; Ar–C, C_6H_5), 121.8 (s; Ar–CH, C_6H_5), 122.2 (s; Ar–CH, Dipp), 124.5 (s; Ar–CH, C_6H_5), 126.0 (s; Ar–C, Dipp), 127.3 (s; Ar–CH, C_6H_5), 129.7 (s; Ar–C, Dipp), 131.4 (s; Ar–CH, Dipp), 141.8, 157.1 (s; C≡C), 177.7 ppm (s; NC(H)N): elemental analyses calculated (%) for $C_{69}H_{91}N_4NdO$ (1136.70): C 72.91; H 8.07; N 4.93; found: C 72.48, H 7.85, N 5.15.

[Sm(DippForm)$_2$(CCPh)(thf)]·toluene (9Sm): A toluene (10 mL) solution of bis(phenylethynyl)mercury (0.21 g, 0.50 mmol) was added dropwise to a stirred deep green toluene (40 mL) solution of [Sm(DippForm)$_2$(thf)$_2$] (1.02 g, 1.00 mmol). After a period of 10 min the solution colour had subsided to yield a pale yellow reaction mixture. Concentration (10 mL) under reduced pressure, followed by standing for three days at ambient temperature yielded **9Sm** as colourless crystals (yield: 0.88 g, 77%). M.p.118–122 °C; IR (Nujol): $\tilde{\nu}$ = 2053 (w), 1666 (m), 1593 (w), 1520 (s), 1317 (m), 1278 (m), 1192 (m), 1098 (w), 1018 (m), 942 (w), 866 (w), 800 (m), 755 (m), 692 cm^{-1} (w); ^{1}H NMR (200.13 MHz, C_6D_6, 333 K): δ = 0.84 (d, ^3J = 6.48 Hz, 48H; CH_3, *i*Pr), 1.04 (m, 4H; THF), 1.18 (m, 4H; THF), 2.11 (s, 3H; CH_3, toluene), 3.08 (m, 8H; CH, *i*Pr), 6.95–7.32 (m, 22H; $4C_6H_3 + 2C_6H_5$), 12.04 ppm (s, 2H; ArNC(H)NAr); elemental analyses calculated (%) for $C_{62}H_{83}N_4SmO$ (no toluene of crystallisation, 1050.68): C 70.74; H 8.14; N 5.32; Found: C 70.21; H 8.07; N 5.00.

X-ray diffraction structure determination: Crystalline samples were mounted in viscous hydrocarbon oil on glass fibres. Crystal data were obtained on an Enraf-Nonius Kappa CCD diffractometer. X-ray data were processed with the DENZO program.[40] Structural solutions and refinements were carried out using SHELXL[41] with the graphical interface X-Seed.[42] All hydrogen atoms excepting the hydroxyl hydrogen of **1YbOH** were placed in calculated positions using the riding model. The hydroxide hydrogen of **1YbOH** (H(1A)) was refined isotropically. Crystal data and refinement parameters are compiled in Table 2 with selected bond lengths and angles provided in Tables 3 (**1Ln–5Ln**), 4 (**6Ln**) and 5 (**9Ln**).

CCDC-651750–651769 contain the supplementary crystallographic data for this paper. These data can be obtained free of charge from The Cambridge Crystallographic Data Centre via www.ccdc.cam.ac.uk/data_request/cif.

*Details for **1La***: One *o*-tolyl group (C(3)–C(9)) and two carbon atoms of a THF donor (C(26) and C(27)) displayed disorder. The disorder was successfully modelled over two sites of partial occupancy with 61:39 and 55:45% occupancy, respectively. Further to this, the THF of solvation displayed a complex disorder, wherein one THF molecule (that of O(2)) resides on a coincident position that overlaps with a second lattice THF molecule located on a special position (O(3), $^1/_2$ in the asymmetric unit and close to inversion centre). This necessitated 1.25 lattice THF molecules per asymmetric unit (2.5 THF molecules per molecular unit). Further disorder was noted for C(33) and C(31A) of THF of solvation. Modelling of disorder failed.

*Details for **1Yb***: One *o*-TolForm ligand exhibited disorder of both N-substituents (that of N(3)C(2)N(4)). N(3) *o*-Tolyl group (C(18)–C(23)) was modelled successfully with 65:35% occupancy over two sites. Disorder of the N(4) *o*-tolyl group was attempted but was unsuccessful. All hydrogen atoms were placed in calculated positions with the exception of those coincident with disordered methyl groups of N(3) *o*-tolyl group.

*Details for **1YbOH***: Two regions of unrefined electron density were located proximal to Yb(1); 3.58 e Å^{-3} at 0.839 Å and 3.05 e Å^{-3} at 0.745 Å.

*Details for **2La***: The disorder of one methylene of a coordinated THF (C(53)), and one methylene and the oxygen of a THF of solvation (C(62) and O(3)) were successfully modelled over two sites of partial occupancy. Occupancies: 69:31, 62:38 and 64:36% respectively.

*Details for **3Nd***: Data were of poor quality with significant disorder identified, but unsuccessfully modelled. ISOR (0.01) refinement was used to obtain satisfactory thermal parameters for all four toluene molecules of solvation.

*Details for **4La***: The disorder of four EtForm methyl groups (C(11), C(23), C(51) and C(61)) was successfully modelled over two sites of partial occupancy. Occupancies: 72:28, 56:44, 80:20 and 75:25% respectively. Modelling of analogous disorder for C(53) failed to provide satisfactory thermal parameters.

*Details for **4Nd***: The disorder of three EtForm methyl groups (C(11), C(23) and C(61)) was successfully modelled over two sites of partial occupancy. Occupancies: 81:19, 61:39 and 69:31% respectively.

*Details for **4Sm***: The disorder of one EtForm methyl group (C(61)) and one THF methylene group (C(69)) were successfully modelled over two sites of partial occupancy (75:25 and 56:44%, respectively). Disorder to C(23) was noted, but modelling proved unsuccessful.

*Details for **4Ho***: The disorder of two EtForm methyl groups C(23) and C(61) was modelled successfully with 63:37% occupancy in both cases. Disorder of a lattice THF molecule was noted (that of O(2)), but modelling failed to provide satisfactory thermal parameters.

*Details for **4Yb***: The disorder of one EtForm methyl group (C(61)) was modelled successfully (65:35%). Regions of unrefined electron density >2 e Å^{-3} were located <1 Å from Yb(1). All other electron density >1 e Å^{-3} was also proximal to Yb(1).

*Details for **6Nd***: The disorder of the isopropyl methyl groups (C(10)) C(11) and C(12)) was modelled over two sites of partial occupancy (60:40%).

*Details for **6Tm***: Regions of unrefined electron density of 1–2 e Å^{-3} were located proximal to Tm(1). All other residual electron density was <1 e Å^{-3}.

*Details for **9Sm***: All regions of unrefined electron density >1 e Å^{-3} were located proximal to Sm(1).

Acknowledgement

The authors would like to thank the Australian Research Council (ARC) for financial support.

[1] a) R. Kempe, *Angew. Chem.* **2000**, *114*, 478–504, *Angew. Chem. Int. Ed.* **2000**, *39*, 468–493; b) P. W. Roesky, *Chem. Soc. Rev.* **2000**, *29*, 335–345; c) W. E. Piers, D. J. H. Emslie, *Coord. Chem. Rev.* **2002**, *233*, 131–155; d) F. T. Edelmann, D. M. M. Freckmann, H. Schumann, *Chem. Rev.* **2002**, *102*, 1851–1896; e) S. Cotton, in *Comprehensive Coordination Chemistry II, Vol. 3* (Eds.: J. A. McCleverty, T. J. Meyer, G. F. R. Parkin), Elsevier, Oxford, **2004**, Chapter 3.2, pp. 93–188; f) R. Anwander, *Top. Curr. Chem.* **1996**, *179*, 33–112; g) F. T. Edelmann, *Coord. Chem. Rev.* **1994**, *137*, 403–481; h) F. T. Edelmann, *Top. Curr. Chem.* **1996**, *179*, 113–148; i) F. T. Edelmann, *Adv. Organomet. Chem.* **2007**, in press; j) F. T. Edelmann in *Comprehensive Organometallic Chemistry III, Vol. 4* (Eds.: R. H. Crabtree, D. M. P. Mingos), Elsevier, Oxford, **2006**, pp. 1–190.

[2] a) J. Richter, J. Feiling, H.-G. Schmidt, M. Noltemeyer, W. Brüser. F. T. Edelmann, *Z. Anorg. Allg. Chem.* **2004**, *630*, 1269–1275; b) S. Bambirra, M. J. R. Brandsma, E. A. C. Brussee, A. Meetsma, B. Hessen, J. H. Teuben, *Organometallics* **2000**, *19*, 3197–3204.

[3] M. L. Cole, P. C. Junk, *Dalton Trans.* **2003**, 2109–2111.

[4] P. C. Junk, M. L. Cole, *Chem. Commun.* **2007**, 1579–1590.

[5] a) L. Luo, Y. Yao, Q. Shen, J. Sun, L. Wang, *J. Organomet. Chem.* **2002**, *662*, 144–149; b) L. Zhou, Y. Yao, Y. Zhang, M. Xue, J. Chen, Q. Shen, *Eur. J. Inorg. Chem.* **2004**, 2167–2172; c) J.-L. Chen, Y.-M. Yao, Y.-J. Luo, L.-Y. Zhou, Y. Zhang, Q. Shen, *J. Organomet. Chem.* **2004**, *689*, 1019–1024; d) Y. Zhou, G. P. A. Yap, D. S. Richeson, *Organometallics* **1998**, *17*, 4387–4391.

[6] a) G. B. Deacon, C. M. Forsyth, S. Nickel, *J. Organomet. Chem.* **2002**, *647*, 50–60; b) G. B. Deacon, C. M. Forsyth, in *Inorganic Chemistry Highlights*, (Eds.: G. Meyer, D. Naumann, L. Wesemann), Wiley-VCH, Germany, Weinheim, **2002**, Chapter 7, pp. 139–153; c) K. Müller-Buschbaum, *Z. Anorg. Allg. Chem.* **2005**, *631*, 811–828.

[7] R. M. Roberts, *J. Am. Chem. Soc.* **1949**, *71*, 3848–3849.

[8] M. L. Cole, P. C. Junk, *Chem. Commun.* **2005**, 2695–2697.

[9] G. B. Deacon, G. D. Fallon, C. M. Forsyth, S. C. Harris, P. C. Junk, B. W. Skelton, A. H. White, *Dalton Trans.* **2006**, 802–812.

[10] M. L. Cole, G. B. Deacon, P. C. Junk, K. Konstas, *Chem. Commun.* **2005**, 1581–1583.

[11] a) J. L. Kiplinger, T. G. Richmond, C. L. Osterberg, *Chem. Rev.* **1994**, *94*, 373–431; b) J. Burdenuic, B. Jedlicka, R. H. Crabtree, *Chem. Ber./Recl.* **1997**, *130*, 145–154; c) H. Dorn, E. F. Murphy, S. A. A. Shah, H. W. Roesky, *J. Fluorine Chem.* **1997**, *86*, 121–125.

[12] For examples see: a) C. J. Burns, D. J. Berg, R. A. Andersen, *J. Chem. Soc. Chem. Commun.* **1987**, 272–273; b) C. J. Burns, R. A. Andersen, *J. Chem. Soc. Chem. Commun.* **1989**, 136–137; c) P. L. Watson, T. H. Tulip, I. Williams, *Organometallics* **1990**, *9*, 1999–2009; d) G. B. Deacon, S. C. Harris, G. Meyer, D. Stellfeldt, D. L. Wilkinson, G. Zelesny, *J. Organomet. Chem.* **1998**, *552*, 165–170; e) G. B. Deacon, G. Meyer, D. Stellfeldt, *Eur. J. Inorg. Chem.* **2000**, 1061–1071; f) H. Schumann, M. R. Keitsch, J. Winterfeld, J. Demschuk, *J. Organomet. Chem.* **1996**, *525*, 279–281.

[13] For recent examples where a trivalent precursor is used to generate a heteroleptic lanthanoid fluoride see: a) Z. Xie, K. Chui, Q. Yang, T. C. W. Mak, J. Sun, *Organometallics* **1998**, *17*, 3937–3944; b) W. J. Evans, D. G. Giarikos, M. A. Johnston, M. A. Greci, J. W. Ziller, *J. Chem. Soc. Dalton Trans.* **2002**, 520–526; c) L. Maron, E. L. Werkema, L. Perrin, O. Eisenstein, R. A. Andersen, *J. Am. Chem. Soc.* **2005**, *127*, 279–292.

[14] For a recent extensions of the divalent oxidation state to several lanthanoid elements see: a) M. N. Bochkarev, *Coord. Chem. Rev.* **2004**, *248*, 835–851; b) W. J. Evans, *J. Organomet. Chem.* **2002**, *647*, 2–11; c) W. J. Evans, N. T. Allen, P. S. Workman, J. C. Meyer, *Inorg. Chem.* **2003**, *42*, 3097–3099; d) W. J. Evans, D. S. Lee, D. B. Rego, J. M. Perotti, S. A. Kozimor, E. K. Moore, J. W. Ziller, *J. Am. Chem. Soc.* **2004**, *126*, 14574–14582; e) M. C. Cassani, D. Duncalf, M. F. Lappert, *J. Am. Chem. Soc.* **1998**, *120*, 12958–12959; f) F. Jaroschik, F. Nief, X.-F. Le Goff, L. Ricard, *Organometallics* **2007**, *26*, 1123–1125; g) F. Nief, D. Turcitu, L. Ricard, *Chem. Commun.* **2002**, 1646–1647; h) W. J. Evans, *Inorg. Chem.* **2007**, *46*, 3435–3449.

[15] K. P. Butin, A. N. Kashin, I. P. Beletskaya, L. S. German, V. R. Polishchuk, *J. Organomet. Chem.* **1970**, *25*, 11–16.

[16] G. B. Deacon, D. L. Wilkinson, *Inorg. Chim. Acta* **1988**, *142*, 155–159.

[17] G. B. Deacon, A. J. Koplick, W. D. Raverty, D. G. Vince, *J. Organomet. Chem.* **1979**, *182*, 121–141.

[18] G. B. Deacon, P. J. MacKinnon, T. D. Tuong, *Aust. J. Chem.* **1983**, *36*, 43–53.

[19] G. B. Deacon, C. M. Forsyth, J. Sun, *Tetrahedron Lett.* **1994**, *35*, 1095–1098.

[20] a) D. E. Fenton, A. G. Massey, *Tetrahedron* **1965**, *21*, 1009–1018; b) D. E. Fenton, A. J. Park, D. Shaw, A. G. Massey, *J. Organomet. Chem.* **1964**, *2*, 437–446; c) D. D. Callander, P. L. Coe, J. C. Tatlow, *Tetrahedron* **1966**, *22*, 419–432; d) S. C. Cohen, A. J. Tomlinson, M. R. Wiles, A. G. Massey, *J. Organomet. Chem.* **1968**, *11*, 385–392.

[21] P. L. Coe, R. Stephens, J. C. Tatlow, *J. Chem. Soc.* **1962**, 3227–3231.

[22] A. J. Tomlinson, A. G. Massey, *J. Organomet. Chem.* **1967**, *8*, 321–327.

[23] G. Massarweh, R. D. Fischer, *J. Organomet. Chem.* **1993**, *444*, 67–74.

[24] a) W. J. Evans, J. T. Leman, J. W. Ziller, S. I. Khan, *Inorg. Chem.* **1996**, *35*, 4283–4291; b) H. Schumann, M. Glanz, H. Hemling, F. H. Gorlitz, *J. Organomet. Chem.* **1993**, *462*, 155–161; c) W. J. Evans, T. A. Ulibarri, L. R. Chamberlain, J. W. Ziller, D. Alvarez, *Organometallics* **1990**, *9*, 2124–2130.

[25] G. B. Deacon, T. Feng, C. M. Forsyth, A. Gitlits, D. C. Hockless, Q. Shen, B. W. Skelton, A. H. White, *J. Chem. Soc. Dalton Trans.* **2000**, 745–751.

[26] G. B. Deacon, A. J. Koplick, T. D. Tuong, *Aust. J. Chem.* **1984**, *37*, 517–525.

[27] H. Noss, W. Baumann, R. Kempe, T. Irrgang, A. Schults, *Inorg. Chim. Acta* **2003**, *345*, 130–136.

[28] R. D. Shannon, *Acta Crystallogr. Sect. A* **1976**, *32*, 751–767.

[29] P. B. Hitchcock, M. F. Lappert, S. Prashar, *J. Organomet. Chem.* **1991**, *413*, 79–90.

[30] G. B. Deacon, G. Meyer, D. Stellfeldt, G. Zelesny, B. W. Skelton, A. H. White, *Z. Anorg. Allg. Chem.* **2001**, *627*, 1652–1658.

[31] S. Bambirra, A. Meetsma, B. Hessen, *Organometallics* **2006**, *25*, 3454–3462.

[32] C. L. Beswick, J. M. Schulman, E. I. Stiefel, *Prog. Inorg. Chem.* **2003**, *52*, 55–110; provides a more detailed description of twisting from octahedral to trigonal prismatic stereochemistry.

[33] C. Villers, P. Thuèry, M. Ephritikhine, *Eur. J. Inorg. Chem.* **2004**, 4624–4632.

[34] D. M. Barnhart. D. L. Clark, J. C. Gordon, J. C. Huffman, R. L. Vincent, J. G. Watkin, B. D. Zwick, *Inorg. Chem.* **1994**, *33*, 3487–3497.

[35] G. B. Deacon, T. Feng, B. W. Skelton, A. H. White, *Aust. J. Chem.* **1995**, *48*, 741–756.

[36] A. C. Hillier, X. W. Zhang, G. H. Maunder, S. Y. Liu, T. A. Eberspacher, M. V. Metz, R. McDonald, A. Domingos, N. Marques, V. W. Day, A. Sella, J. Takats, *Inorg. Chem.* **2001**, *40*, 5106–5116.

[37] S. Beaini, G. B. Deacon, M. Hilder, P. C. Junk, D. R. Turner, *Eur. J. Inorg. Chem.* **2006**, 3434–3441.

[38] a) G. B. Deacon, A. J. Koplick, W. D. Raverty, D. G. Vince, *J. Organomet. Chem.* **1979**, *182*, 121–141; b) M. N. Bochkarev, V. V. Khramenkov, Y. F. Rad′kov, L. N. Zakharov, Y. T. Struchkov, *J. Organomet. Chem.* **1992**, *429*, 27–39; c) L. N. Bochkarev, T. A. Stepantseva, L. N. Zakharov, G. K. Fukin, A. I. Yanovsky, Y. T. Struchkov, *Organometallics* **1995**, *14*, 2127–2129; d) G. B. Deacon, C. M. Forsyth, P. C. Junk, unpublished results.

[39] a) G. B. Deacon, J. E. Cosgriff, E. T. Lawrenz, C. M. Forsyth, D. L. Wilkinson, in *Herrmann-Brauer, Synthetic Methods of Organometallic and Inorganic Chemistry, Vol. 6* (Ed.: W. A. Herrmann), Thieme, Stuttgart, **1997**, p. 48; b) R. Johnson, W. L. McEwan, *J. Am. Chem. Soc.* **1926**, *48*, 469–476.

[40] Z. Otwinowski, W. Minor, *Methods Enzymol.* **1997**, *276*, 307–326.

[41] G. M. Sheldrick, SHELXL-97, University of Göttingen, Germany, **1997**.

[42] L. J. Barbour, *J. Supramol. Chem.* **2001**, *1*, 189–191.

Received: June 25, 2007
Published online: September 4, 2007

